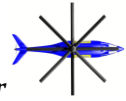


28th Annual AHS Student Design Competition

Undergraduate Category





Acknowledgements

We would like to recognize and thank the following individuals for their assistance in the completion of this design project:

Dr. Daniel Schrage

Mr. Alek Gavrilovski

Dr. Robert G. Loewy

Ms. Ritu Marpu

Dr. Lakshmi Sankar

Mr. Marc Mugnier

Dr. Kyle Collins

Mr. Ersel Olcer

Dr. B.Y. Min

Mr. Alex Robledo

Mr. Jeremy Bain

Mr. Robert Scott

2011 Georgia Tech Undergraduate Design Team

Handwritten signature of Laura Armanios in black ink.

Laura Armanios (Senior, GaTech)

Handwritten signature of Silvio Lopez in black ink.

Silvio Lopez (Senior, GaTech)

Handwritten signature of Natasha Barbely in black ink.

Natasha Barbely (Senior, GaTech)

Handwritten signature of Trevor Mohr in black ink.

Trevor Mohr (Senior, GaTech)

Handwritten signature of Andrew T. Carter in black ink.

Andrew Carter (Senior, GaTech)

Handwritten signature of Michael Moyer in black ink.

Michael Moyer (Senior, GaTech)

Handwritten signature of Dennis Garza in black ink.

Dennis Garza (Senior, GaTech)

Handwritten signature of Kit Taylor in black ink.

Kit Taylor (Senior, GaTech)

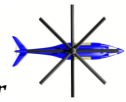
Handwritten signature of Gregg Hines in black ink.

Gregg Hines (Senior, GaTech)

Handwritten signature of Dr. Daniel P. Schrage in black ink.

Dr. Daniel P. Schrage (Principal Advisor)

For participating in the 2011 AHS design competition, undergraduate students received academic credit for AE 4359: Rotorcraft Design.



Executive Summary

The 2011 AHS Student Design Competition calls for an aircraft capable of performing multiple missions. This proposal answers this request with the introduction of the Golden Retriever, a rotorcraft capable of performing primarily search and rescue, resupply, and insertion type missions. Modern day current events call for the need to have an individual rotorcraft able to complete a variety of missions. Events caused by natural disasters where performing search and rescue is just as important as dropping off supplies to a remote area in need of help, would benefit significantly from the Golden Retriever. As another example, the environment needs future rotorcraft to perform more tasks to reduce the negative impact of having multiple rotorcraft in service. The military greatly benefits from a multi mission rotorcraft since deploying with rotorcraft that are capable of accomplishing any mission allows commanders more flexibility.

The Golden Retriever can easily accomplish the types of missions that are most common in today's world. A custom airfoil was designed in order to design the rotor for maximum lift at high speeds. Since this rotorcraft was intended to satisfy the "Golden Hour" requirement for search and rescue missions, aux propulsion was introduced so to ensure high speeds would be possible by unloading the main rotor and providing forward thrust. The aux propulsion prompted the design of a transmission that was capable of delivering power from the engines to both the main rotors and the aux propulsion. The Golden Retriever focused heavily on speed; therefore the fuselage was designed to have as low drag as possible. The cabin was designed with versatility in mind by allowing the use of several configurations within a moment's notice. The Golden Retriever can bring back wounded persons and then go back in a short time and drop off supplies. For those missions performed in hostile environments the Golden Retriever will stay safe thanks to the IR Suppression built into the tailboom. The Golden Retriever utilizes a highly efficient drivetrain that takes in power

The Golden Retriever has good performance at both standard sea level and 6K95. The Golden Retriever is able to perform the critical search and rescue mission with the "Golden Hour" requirement at both conditions. This is still the case even at the Golden Retriever's max gross take off weight.

The design team for the Golden Retriever relied on technical tools and methods to answer the request for a multi mission rotorcraft. Public and commercial software was used to obtain impressive results. The applicable software allowed ideas to be analyzed and proven in order to better the design. Several iterations were performed in the design, feeding back to other factors and adjusting as necessary.

Herein is enclosed the proposal for a multi mission rotorcraft. The design features are highlighted and explained showing the Golden Retriever is capable of becoming the future of rotorcraft.

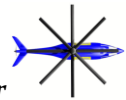
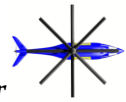
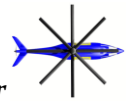


Table of Contents:

ACKNOWLEDGEMENTS.....	ii
TABLE OF CONTENTS.....	iv
LIST OF FIGURES.....	vi
LIST OF TABLES.....	viii
1. INTRODUCTION.....	2
2. REQUIREMENTS ANALYSIS.....	2
2.1. MISSION ANALYSIS.....	2
2.2. MISSION REQUIREMENT ANALYSIS.....	3
3. CONCEPT SELECTION AND SIZING.....	4
3.1. POTENTIAL CONFIGURATIONS.....	4
3.1.1. Conventional Helicopter.....	4
3.1.2. Compound.....	5
3.1.3. Coaxial.....	5
3.1.4. Tilt Rotor.....	5
3.2. CONFIGURATION SELECTION.....	5
3.3. CIRADS SIZING.....	6
4. MAIN ROTOR DESIGN.....	8
4.1. HUB TRADE STUDY.....	8
4.1.1. Articulated Rotor, Swashplate Control.....	8
4.1.2. Bearingless/Hingeless Hub.....	9
4.2. BLADE CONTROL.....	9
4.3. ROTOR DESIGN.....	10
4.3.1. Rotor Diameter.....	10
4.3.2. Tip Speed.....	10
4.3.3. Number of Blades.....	11
4.3.4. Blade Twist/Taper.....	12
4.3.5. Rotor Separation.....	12
4.4. AIRFOIL DESIGN.....	13
4.4.1. Xfoil Validation.....	14
4.4.2. Design Scheme.....	14
4.4.3. DG-12.....	16
4.5. DRAG DIVERGENCE STUDY.....	16
4.6. FINAL AIRFOIL SELECTION.....	18
4.7. NOISE ANALYSIS.....	18
5. FUSELAGE AERODYNAMICS.....	21
6. YAW CONTROL.....	22
6.1. HOVER.....	22
6.2. FORWARD FLIGHT.....	23
6.3. AUTOROTATION.....	23
7. PROPULSION.....	25
7.1. ENGINES.....	25
7.2. IR SUPPRESSION.....	25



7.3. AUXILIARY PROPELLER.....	26
7.3.1. Aux Propeller Thrust Scheduling.....	28
8. DRIVE TRAIN.....	29
8.1. REQUIREMENT.....	29
8.2. CONCEPT SELECTION.....	29
8.2.1. The Concept.....	29
8.3. STRESS ANALYSIS.....	31
8.4. PUSHER.....	32
9. STRUCTURES.....	32
9.1. REQUIREMENTS.....	32
9.2. MATERIAL SELECTION.....	32
9.2.1. Trade Study.....	32
9.2.2. Material Properties.....	33
9.3. COAX STRUCTURAL LAYOUT.....	34
9.3.1. Description of What Coax Includes.....	34
9.3.2.Placements of Parts/Reasoning.....	34
9.4. STRUCTURAL BREAKDOWN.....	35
9.4.1. Forward Fuselage.....	35
9.4.2.Center Fuselage.....	35
9.4.3.Aft Fuselage.....	35
9.4.4. Additional Parts.....	35
9.5. CRASHWORTINESS/FATIGUE.....	35
9.6. FINITE ELEMENTANALYSIS.....	37
10. RECONFIGURABLE CABIN.....	38
11. VEHICLE PERFORMANCE SUMMARY.....	40
12. WEIGHT ANALYSIS.....	43
13. COCKPIT AND CABIN SYSTEMS.....	45
14. COST ANALYSIS.....	46
15. CONCLUSION.....	48



List of Figures

Figure 1: Search and Rescue Mission.....	3
Figure 2: Insertion Mission.....	4
Figure 3: Resupply Mission.....	4
Figure 4: CIRADS Mission Sizing.....	7
Figure 5: CIRADS Vehicle Sizing.....	7
Figure 6: Hub Design Prioritization Matrix.....	8
Figure 7: Kamov Style Articulated Rotor.....	8
Figure 8: Sikorsky X2 Bearingless Hub.....	9
Figure 9: Kamov Ka-52.....	9
Figure 10: Sikorsky X2.....	10
Figure 11: Radius Sizing of Rotor with Respect to DL.....	10
Figure 12: Tip Speed vs. Blade Span Analysis.....	11
Figure 13: Blade Twist and Taper.....	12
Figure 14: Rotor Separation Graphical Representation.....	13
Figure 15: Validation of AG38 Airfoil vs. Wind Tunnel Data.....	14
Figure 16: Comparison of 1/MSD for the Airfoil Shapes Under Consideration.....	15
Figure 17: Modified and Baseline Airfoils.....	16
Figure 18: Drag Coefficient (left) and Slope (right) of Drag vs. Mach Number.....	16
Figure 19: Series of Mach Numbers Showing Drag Divergence.....	17
Figure 20: Main Rotors and Aux Prop Inputted into PSU-WOPWOP.....	19
Figure 21: Two Rotor Radiuses Away from Center of Main Rotor.....	20
Figure 22: Location of Microphones.....	20
Figure 23: Streamlines Around the Fuselage of the Golden Retriever.....	22
Figure 24: Surface Pressure Coefficient Contours Over the Golden Retriever Fuselage.....	22
Figure 25: Weight Versus Power.....	25

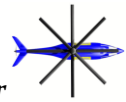
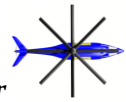
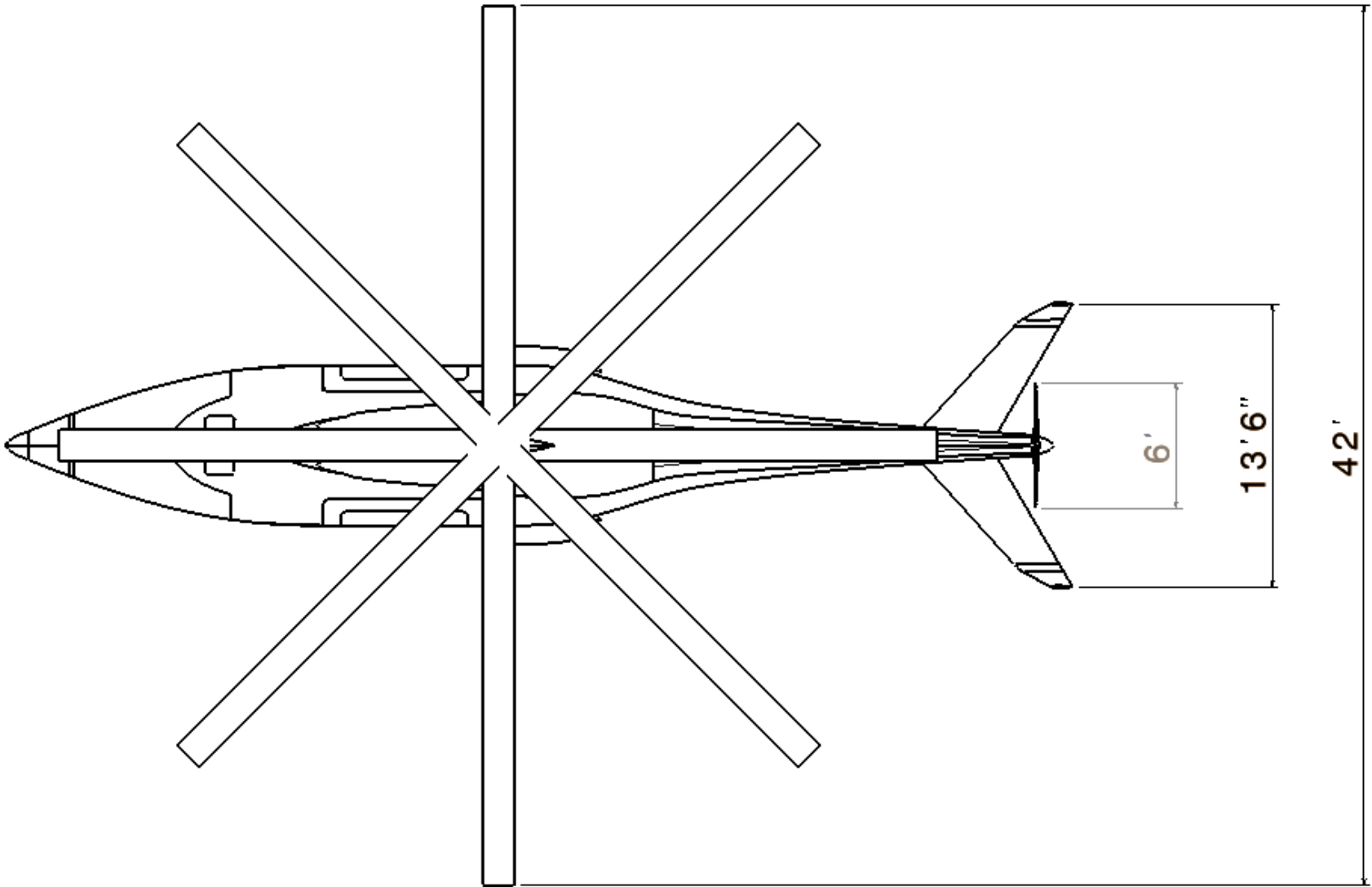
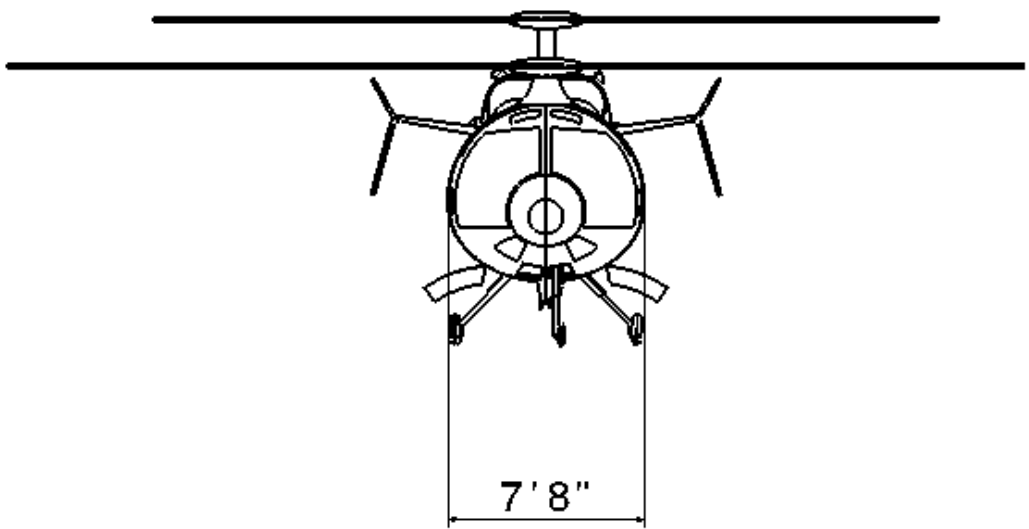
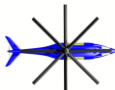


Figure 26: SFC Versus Power.....	25
Figure 27: Exhaust.....	26
Figure 28: Aux Propeller AC2011.....	26
Figure 29: Power Required Versus Thrust.....	27
Figure 30: Aux Power Required vs. Forward Flight Speed at Sea Level.....	28
Figure 31: Drive Train Schematic.....	30
Figure 32: CAD Rendering of Main Rotor Transmission.....	30
Figure 33: Transmission Stress Analysis.....	33
Figure 34: Primary Structural Breakdown.....	34
Figure 35: Finite Element Model.....	37
Figure 36: ABAQUS Drop Test Layout.....	38
Figure 37: Mission 1 Layout.....	38
Figure 38: Mission 2 Configuration Option A.....	39
Figure 39: Mission 2 Configuration B.....	39
Figure 40: Mission 3 Configuration.....	40
Figure 41: Validation of Power Required Code.....	41
Figure 42: Power Required at Sea Level.....	42
Figure 43: Power Required at 6K95.....	42
Figure 44: CIRADS Weight Breakdown.....	43
Figure 45: Insertion Mission Weight Percentages.....	45



List of Tables

Table 1: Team Requirements Analysis	2
Table 2: Current Vertical Lift Aircraft Ship Board Capable.....	3
Table 3: Configuration Selection	5
Table 4: Morphological Matrix.....	6
Table 5: High Rotor Tip Speed Analysis	11
Table 6: Assumptions Made For Blade Twist/Taper Optimization	12
Table 7: Blade Droop Analysis.....	13
Table 8: Airfoil Shapes Considered for Optimization	15
Table 9: Noise Analysis Results	21
Table 10: Equivalent Flat Plate Drag of Each Component of the Golden Retriever	21
Table 11: Equivalent Flat Plate Drag of Each Component of the Lynx Mk 7.....	21
Table 12: Considered Methods for Supplementing Yaw Controls	24
Table 13: GE-CT7-8A Parameters per Engine	25
Table 14: Pusher Propeller Parameters	27
Table 15: Aux Propeller Thrust Scheduling	28
Table 16: Transmission Gear Specs.....	31
Table 17: T300/976 Graphite/Epoxy Properties	33
Table 18: Nomex Honeycomb Core Properties	33
Table 19: Weight Buildup.....	44
Table 20: Cost Analysis	46



Empty Weight - 11689 lbs

Max GW - 18000 lbs

Max Payload - 4000 lbs

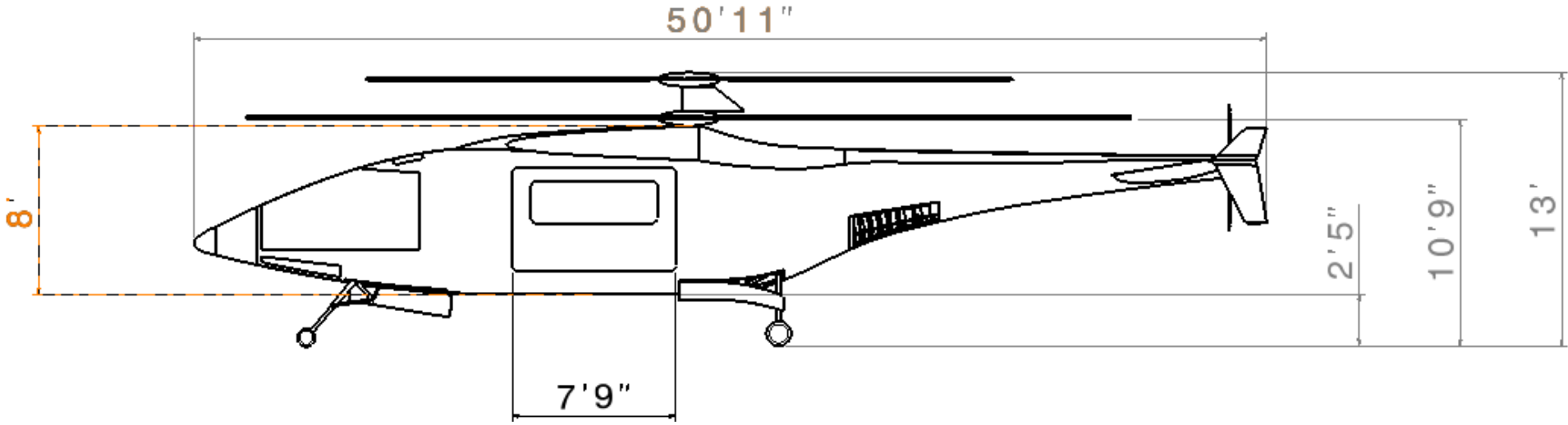
Fuel - 2360 lbs

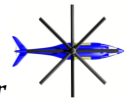
Max Range - 518 nm

Max Endurance - 4.5 hrs

Max Cruise Airspeed - 249 knots

Max Dash Airspeed - 260 knots





1. Introduction

The Bell Helicopter sponsored 28th Annual AHS Student Design Competition requests a new vertical lift system with increased versatility and capable of performing multiple types of missions. This proposal describes the Golden Retriever; a vertical lift rotorcraft capable of performing search and rescue, insertion, and resupply missions easily and effectively. The Golden Retriever is designed to operate in extreme conditions while still being able to perform the required range of missions. No detail has been overlooked in the design of this year's solution to the Request For Proposal (RFP).

Due to today's demands for faster, stronger and more efficient vertical lift aircraft, modern day multi mission vertical lift aircraft are in dire need of an overhaul. This report describes the design process of the Golden Retriever from conceptual to preliminary design. Many factors were studied carefully, however much attention was placed into specific key innovations. The design team strongly feels the requirements should not only be met, but exceeded. When produced, the Golden Retriever will be an important player in the battlefield or at home.

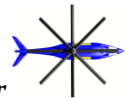
2 Requirements Analysis

As with any design, understanding the requirements was the first step in the design process. The design team gathered the explicit information listed in the RFP and then noted the requirements. The individual missions were then analyzed to understand how the vehicle is expected to perform.

2. 1 Design Requirement Analysis

Table 1 Team Requirements Analysis

Requirement	Target	Tools used
AHS Explicit Requirements		
VTOL Capability	VTOL	Design
Reconfigurable Cabin	1 hr	CATIA
Rubber CT7-8A Engine	Rubber CT7-8A Engine	Matlab
ICAO Level 4 noise requirements	Level 4	WopWop/GT-Hybrid
Team Requirements		
Operability	3 times a week	Design
Crew members	4	Design
Reserve Fuel FAR	45 minutes	CIRADS, Matlab
Streamline fuselage	Retractable landing gear	CATIA
Minimum Range	550 nm	Excel
Max Speed	225 knots	Excel
One Engine Inoperative	Hover at Sea Level with one engine	Excel
Autorotative Index	25	Matlab



2.2 Mission Requirement Analysis

This year’s RFP specifically calls for a multi-mission vehicle, with the ability to execute three specific missions to reduce the need for multiple types of vehicles. This in turn reduces component inventory and maintenance costs due to the commonality of parts. A perfect example of where a multi-mission vehicle will be very beneficial is on an amphibious assault ship. A modern day American amphibious assault ship carries up to five different vertical lift vehicles. They are listed in Table 2 with their respective mission. With a multi mission vehicle aboard the ship, there would only be a need for four different vertical lift vehicles.

Table 2 Current vertical lift aircraft ship board capable

Aircraft	Primary Mission
AV-8 Harrier	Light Attack
CH-46	Transport
CH-53	Heavy Lift
UH-1N	Emergency Evacuation
AH-1W	Close Air Support

The multi-mission vehicle can take the place of the CH-46 and UH-1N thus simplifying the logistics of stocking spare parts on the ship.

Figure 1 Figure 1 Search and Rescue Mission draws out the mission profile for Mission 1, the Search and Rescue mission. This mission’s limiting factor is the stringent speed requirement. Because Mission 1 is a search and rescue mission and the RFP requires the patients to be brought to medical attention within an hour of pickup (Golden Hour), the rotorcraft must travel at speeds in excess of 225 knots.

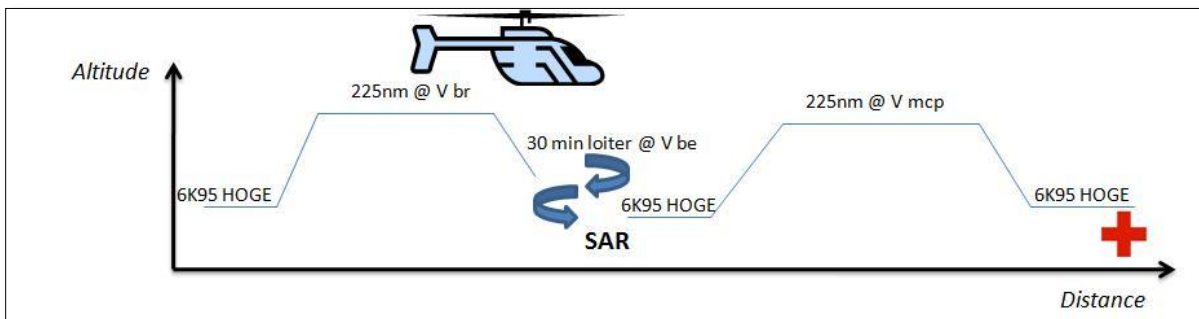


Figure 1 Search and Rescue Mission

Mission 2 and Mission 3 are quite similar when comparing their profiles. The only difference between these two missions is the payload they carry. In Mission 2 the payload is 4,000 lbs worth of troops and their gear. The insertion mission only requires that there be payload on the inbound leg. The resupply mission takes 3,000 lbs worth of supplies to drop off and then pickups 3,000 lbs for the return flight. Figure 2 and Figure 3 draw out the profile for Missions 2 and 3.

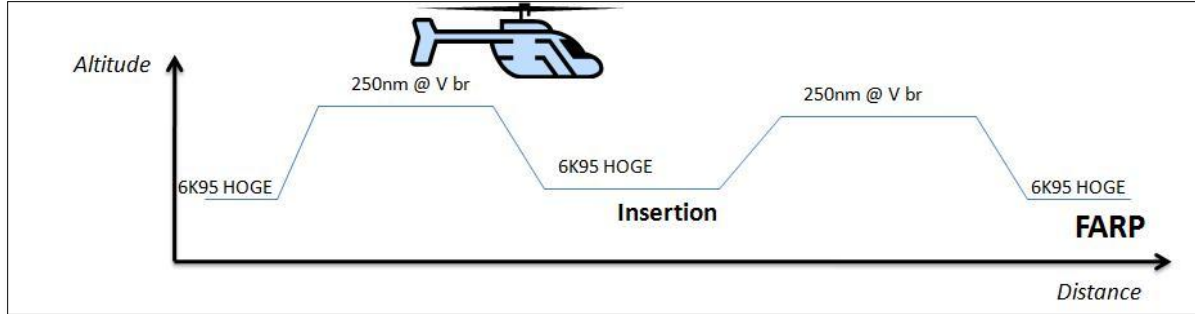
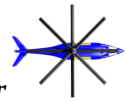


Figure 2 Insertion Mission

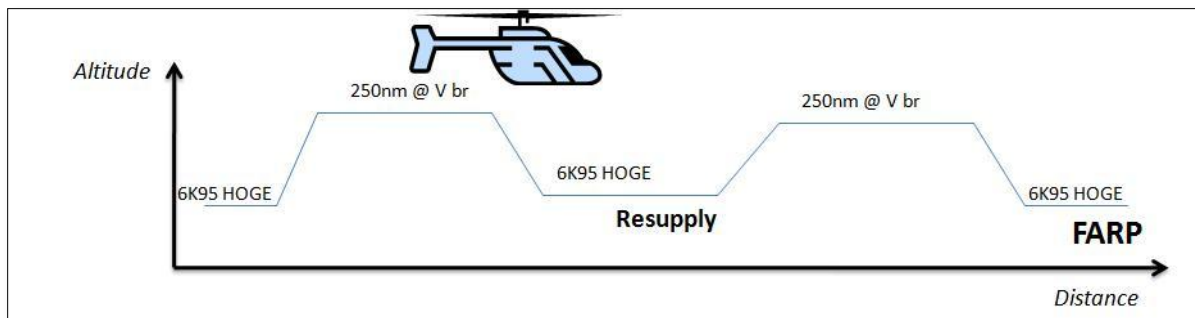


Figure 3 Resupply Mission

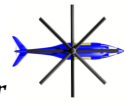
3. Concept Selection and Sizing

With a better understanding of the requirements at hand, the team began the process of conceptual design selection. This process allowed a configuration to be determined, evaluated, and eventually sized to the specific missions. The sizing of the vehicle was done with CIRADS, where an empty weight of the vehicle was obtained.

3.1 Potential Configurations

3.1.1 Conventional Helicopter

The UH-60 Blackhawk by Sikorsky was first analyzed. This aircraft is the modern day multi mission rotorcraft; however it does not meet the mission requirements specified in the RFP. With the UH-60 being a conventional rotorcraft, it is very unlikely this configuration would be able to meet the stringent requirement of 225 knots for Mission 1. The UH-60 has a max speed of 159 knots and would need several modifications and adjustments to increase its speed.



3.1.2 Compound Helicopter

A compound helicopter like the X-49 Speedhawk by Piasecki will be better able to meet the speed requirement of Mission 1. Unloading the main rotor and applying external thrust is an extremely effective way of reaching high speeds without compromising vertical lift. The X-49 also has the configuration to be able to perform an insertion and resupply mission. Unfortunately, the X-49 has fixed wings on the sides of the fuselage. The downfall of this is the extra download in hover and the inconvenience of entering and exiting the rotorcraft with the wings in the way. Because this is a multi-mission aircraft, reconfiguring the aircraft for each different mission in a timely manner is crucial.

3.1.3 Coaxial Helicopter

With the latest advancements made by Sikorsky with the X2, there is no doubt a coaxial helicopter will be able to meet the speed requirements of Mission 1. With advancements in materials, the droop of the main rotor blade has been reduced, thus allowing the minimization of the separation of the rotors for further reduction in hub drag. The X2 does lack heavily on cargo space since there is no cabin. The coaxial helicopters that are capable of carrying cargo however are extremely poor in aerodynamic efficiency. The Russian Kamov's are a good example of these coaxial helicopters with their articulated rotors.

3.1.4 Tilt Rotor

The tilt rotor aircraft is capable of reaching high speeds when compared to the conventional helicopter and can carry large payloads. Due to high disk loading, the tilt rotor is not very efficient in hover or when having to loiter as would be needed for the search and rescue mission.

3.2 Configuration Selection

After looking into the different concepts, they were analyzed by the team quantitatively. Table 3 lists the advantages/disadvantages of each concept as seen by the team. From comparing all of the configurations, it was found that the coaxial concept would be the best candidate to meet the requirements. In order to properly consider and evaluate possible configurations for the coaxial concept, the team created a morphological matrix. The physical making of what would be the VTOL aircraft was used to construct the matrix. For each subsystem, a few alternatives were considered and from this the final configuration was collectively decided on

Table 3 Configuration Selection

Configuration	Advantage	Disadvantage
Conventional Helicopter	Very popular	Not capable of high speeds
Compound	Easier to unload main rotor	High empty weight fraction
Coaxial	Capable of high speeds	Very complex main rotor systems
Tiltrotor	Easily reach high altitude and speeds	Poor efficiency in hover

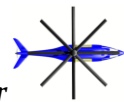


Table 4 Morphological Matrix

Subsystem		Alternatives			
		1	2	3	4
Airframe	Cockpit	Tandem	2 abreast		
	Gear	Retractable	Non-Retractable		
	Wing	Low	High	Stowable	None
	Tail	T-Tail	H-Tail	Dihedral H-Tail	
	Material	Aluminum	Composite		
Powerplant	Engine	Turboshaft	Turboprop	Turbofan	
	Xmsn	Split Torque	Planetary	Hybrid	
Avionics	Control	Hydraulic	Fly-by-wire	Fly-by-light	
	Navigation	VOR/GPS	VOR/ILS/GPS	ILS/GPS	
Lift/Thrust	M/R system	Conventional	Coax	Tandem	Tilt Rotor
	M/R Blades	2	3	4	5
	M/R Hub	Fully Articulated	Hingeless	Bearingless	
	Anti-torque	N/A	Tail rotor	Notar	
	Aux Fwd. Thrust	Puller	Pusher	Turboprop	Turbojet
	Aux Prop. Position	Fuselage	Wings	Tail	

Table 4 highlights the design selected among all the possible alternatives. To briefly summarize the selections, the cockpit will have the setup for two pilots to sit abreast each other. It was decided a coaxial design would best meet the requirements. The landing gear will be retractable in order to maintain a streamlined fuselage for high speeds. The airframe will be completely made of composite material. The tail will be a H-Tail. The powerplant specified in the RFP, the CT7-8A will be the engine used with a planetary type transmission. A bearingless hub was selected and a pusher prop will be used for auxiliary propulsion which will be located just aft of the tail.

3.3 CIRADS Sizing of Concept Selected

With the overall layout of the concept finalized, the team was ready to formally size the vehicle to the missions required in the RFP. The computer software Concept Independent Rotorcraft Analysis and Design Software, CIRADS, was used to ultimately obtain the important parameters such as empty weight and gross weight. CIRADS allows the user to specify the type of mission the vehicle needs to accomplish via way points and enroute legs. The sizing of the vehicle was done using the convergence of the fuel required ratio and the fuel available ratio, commonly called the RF method. Therefore each mission was created in CIRADS and a preliminary model for the aircraft was also created. Figure 4 is the setup of each mission as modeled in CIRADS.

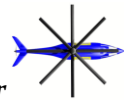


Figure 4 CIRADS Mission Sizing

The next step was to model the aircraft with the minimal inputs needed by CIRADS such as

- Number of Main Rotors
- Disk Loading
- Solidity
- Tip Speed
- Figure of Merit
- Engine Selection
- Equivalent Flat Plate Drag

Other minor inputs and efficiencies were asked by CIRADS, so that one could begin sizing the vehicle to each mission.

The strategy used to properly size the vehicle was to size the vehicle according to the requirements of Mission 2, the Insert/Extract mission. This mission sets the bar for maximum weight needed for the vehicle. Once an empty weight was obtained from this mission, it was used as the starting empty weight for the other missions. The Medevac mission is the most lenient with the weight requirement; however, it is the most demanding on speed. The Resupply mission is very similar to the Insert/Extract mission yet not as demanding. After several iterations, max gross take off weights and fuel weights were obtained for each mission.

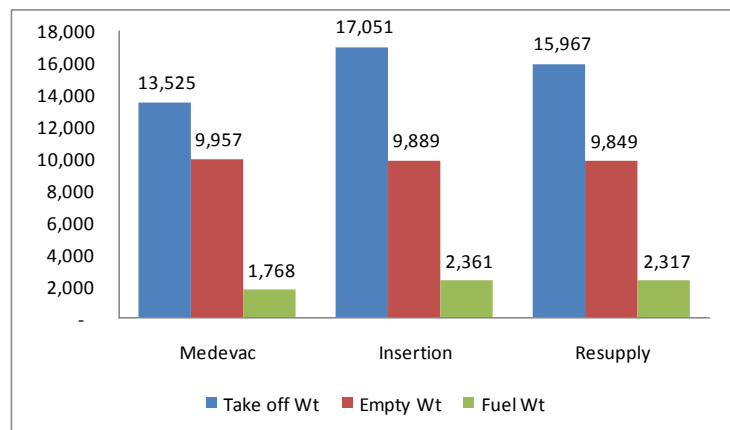
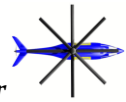


Figure 5 CIRADS Vehicle Sizing



See Figure 5.

From this the vehicle was sized to have an empty weight of 9,957 lbs and a gross weight of 17,051 lbs. The gross weight was rounded up to 18,000 lbs for simplicity and to remain conservative throughout the design process and the empty weight rounded up to 10,000 lbs.

4. Main Rotor Design

4.1 Hub Trade Study

The hub of the rotor was decided to be the first decision made in the process of designing the main rotor. The team ranked the important qualities needed in the hub of the rotor based on the AHS requirements and missions. This was done with a prioritization matrix and using the conservative scale of 1 (much less important), 2, 3, and 6 (very important). The qualities identified for the hub selection were the following in the order of importance: drag, weight, vibrations, safety, maneuverability, noise and maintenance. Results are tabulated in Figure 6.

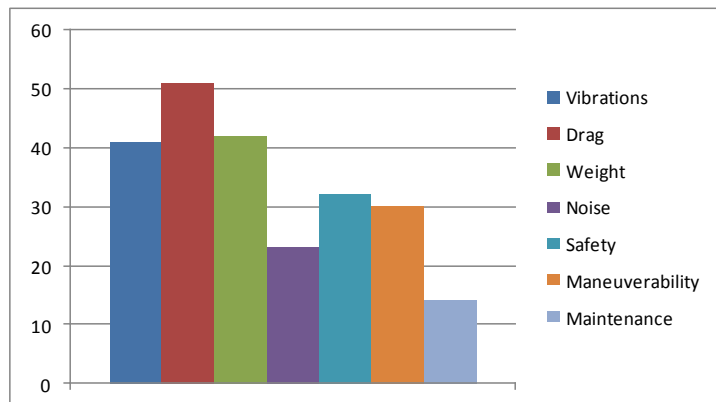


Figure 6 Hub Design Prioritization Matrix

From this the top three qualities for the hub design needs to possess are low drag, weight, and vibrations. Perhaps the driving factor for all of these is the stringent requirement of reaching 225 knots for Mission 1, for which drag and vibrations will be the main obstacles necessary to overcome. For current coaxial applications, there are two designs that are standard, articulated and bearingless with individual blade control.

4.1.1 Articulated Rotor, Swashplate Control

The standard for articulated coaxial helicopters is the three bladed articulated rotor built by Kamov, who have a long history with coaxial helicopters. The well known Ka-50, is capable of reaching speeds near 180 knots. The advantage with this design is the proven experience with coaxial helicopters. However, this complicated design produces a significant amount of drag, and requires a large rotor separation due to the droop of the blades. Figure 7 is a snapshot of the hubs from a Ka-28.

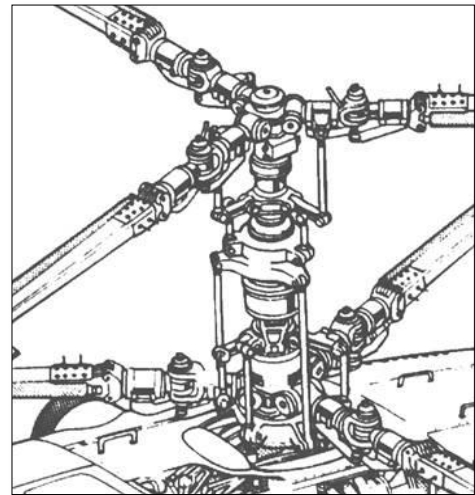
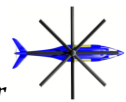


Figure 7 Kamov Style Articulated Rotor



4.1.2 Bearingless/Hingeless Hub

The bearingless hub used by Sikorsky's X2 Technology Demonstrator is shown in Figure 8, which is not a recent advancement. The Sikorsky S-69 pioneered the Advancing Blade Concept (ABC) using hingeless hubs. The advantage of the bearingless/hingeless hub is that it has a stiff in plane rotor. This along with stiff blades minimizes the rotor separation which in turn reduces drag significantly.



Figure 8 Sikorsky X2 Bearingless Hub

4.2 Blade Control

The most common method of blade control for a coaxial rotorcraft is the articulated rotor with swashplate control. However, because the Golden Retriever travels at higher speeds relative to most rotorcraft, this is not the best option. This has relatively high hub drag due to the exposed linkages used to control the blade, as shown in Figure 9.



Figure 9 Komov Ka-52

Because of the increased drag, utilization of a bearingless rotor with individual blade control via hydro-mechanical actuators are employed, which is similar to the Sikorsky X2 and XH-59. Though more expensive, drag in forward flight is significantly reduced because there are far fewer exposed parts. The bearingless hub eliminates the use of any mechanical flap, lead-lag hinges, and feathering bearing. Instead, the degrees of freedom are done via flexures of the hub. Also, similar to the X2, the Golden

Retriever will employ fairings to cover the upper and lower hub to help reduce drag (Figure 10).

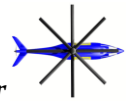


Figure 10 Sikorsky X2

4.3 Rotor Design

4.3.1 Rotor Diameter

The diameter of the rotor was the first parameter to be sized. At this point, the team had a good estimate of the total weight of the vehicle. Calculated was an estimated 18,000lbs for the gross take-off weight (GTOW). Equation 1 was used to properly size the radius of the rotor.

$$R = \frac{1}{\sqrt{2}} \sqrt{\frac{W}{\pi DL}} \quad (1)$$

However, the disk loading (DL) still needed to be determined. After researching several coaxial helicopters, the Kamov Ka-50 was selected to base a similar DL. The Ka-50 was selected because of its high speed capability and similar GTOW. The Ka-50 has a DL of approximately 3.35 lbs/ft² for each rotor. This is the value of DL that was used to calculate the radius of the rotor. Assuming each rotor carries one half the total weight of the aircraft, the radius of each rotor was calculated to be 20.67 ft which was rounded up to 21 ft. Figure 11 shows a graphical representation of equation 1 while varying the DL.

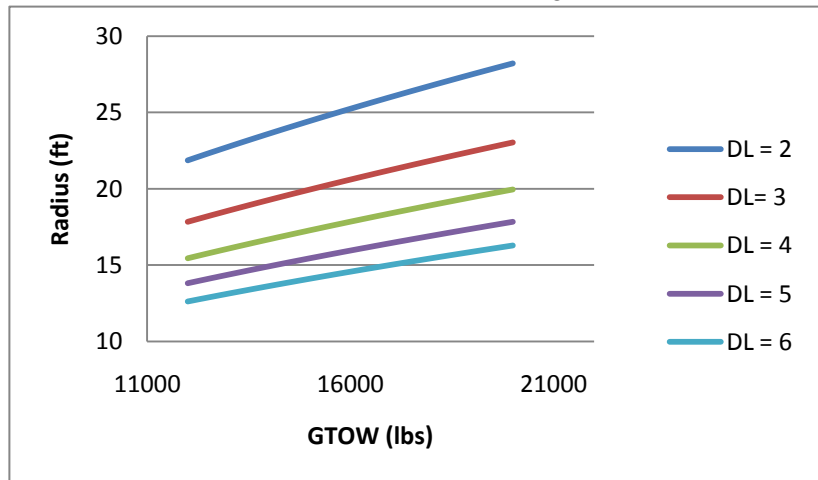


Figure 11 Radius sizing of rotor with respect to DL

4.3.2 Tip Speed

There are many tradeoffs to consider when selecting the tip speed of the rotor. Table 5 identifies the factors that were considered when selecting the tip speed of the rotor.

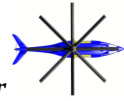


Table 5 High Rotor Tip Speed Analysis

Advantage	Disadvantage
Delay blade stall on retreating blade	Compressibility effects for high V_∞
High stored rotational kinetic energy	Noise
Reduce rotor torque	

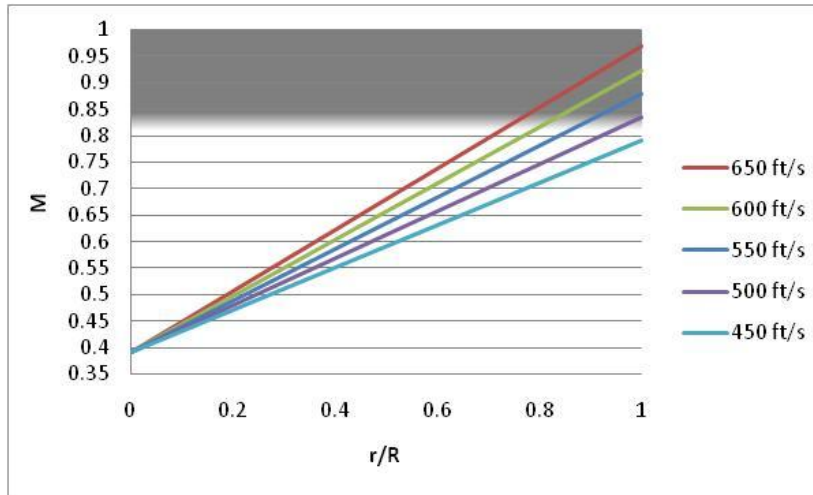


Figure 12 Tip Speed vs. Blade Span Analysis

Compressibility effects could not be accepted for high advance ratios, therefore this is the driving factor for the tip speed selection. A conservative tip speed of 650 ft/s was selected. This tip speed will be set for the zero to 100 knot region of the vehicle.

In order to achieve 225 knots the team quickly realized the advancing blade will travel at a

Mach number of 0.91 at the tip with a tip speed of 650 ft/s, thus encountering critical compressibility effects. Therefore, the tip speed of the rotor needed to be reduced. With the max speed possible taken to be approximately 260 knots, an analysis was done on the span of the blade at this speed to see the Mach number the blade was seeing at various tip speeds. Figure 12 plots these Mach numbers versus the location of the blade at various tip speeds.

Most airfoils have a Mach drag divergence of 0.8 or greater, therefore this region needs to be avoided. One can note that a tip speed of 450 ft/s is just under this region and will be safe at this high speed. Therefore, 450 ft/s is the tip speed of the rotor for the 100 knots condition and above region of the vehicle. This reduction in tip speed will take place in connection with the augmentation of the auxiliary propeller, which is scheduled at 100 knots

4.3.3. Number of Blades

The number of blades was determined by considering the minimization of vibratory loads. Because of the nature of the Medevac mission, being able to provide a smooth ride at high speeds is a necessity. While fewer blades reduce blade and hub weight as well as minimize hub drag, they normally increase the vibration levels at high speeds. Thus, four blades were considered a conservative approach in selecting the number of blades.

4.3.4 Blade Twist/Taper

Having the majority of the key parameters for the rotor, an optimization was needed for the best linear twist of the blade. The team desired to know whether or not twist and taper would benefit the performance of the rotor and if so, by how much. The approach for this trade was to use Blade Element Momentum (BEM) Theory and calculate the figure of merit (FM) while varying the twist and taper simultaneously on the blade. This optimization was done in an Excel environment and made simple assumptions for the rotor. These assumptions are listed in Table 6.

Table 6 Assumptions Made For Blade Twist/Taper Optimization

Parameter	Value
Tip loss factor, B	0.97
Lift curve slope, CL_{α}	5.7 per radian
C_D	$0.0087-0.0216\alpha_{eff}+0.4\alpha_{eff}^2$

By simplifying our equations with these assumptions, the team was able to generate valuable plots that would give an optimal solution for the blade twist and taper. Figure 13 plots the blade twist and taper respectively versus FM.

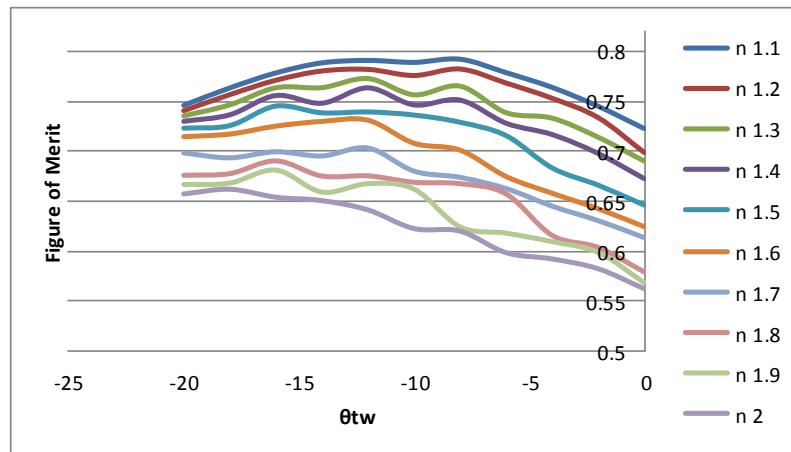


Figure 13 Blade Twist and Taper

From these plots, the optimal blade twist would be -8° . This twist produced a Figure of Merit of 0.792. The optimal taper for the blade was a taper of 1:1. Thus the team will not consider tapering the blades of the rotor. With these optimizations, the team feels confident the main rotors are achieving its maximum performance possible.

4.3.5 Rotor Separation

Simple geometry along with current data was used to calculate the rotor separation for the Golden Retriever. Figure 14 illustrates the layout.

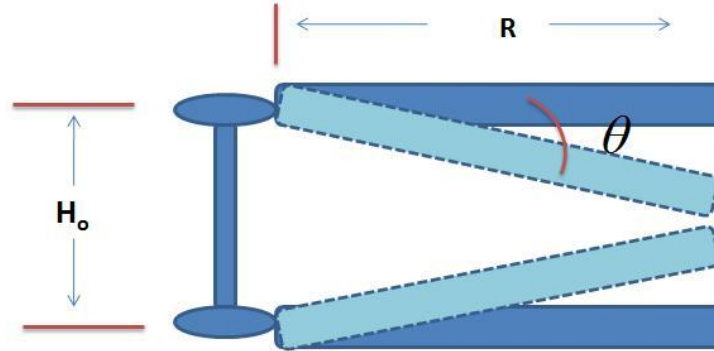
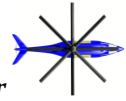


Figure 14 Rotor Separation Graphical Representation

From this equation 2 was derived to calculate the rotor separation, H_o .

$$H_o = [\tan \theta]2R \quad (2)$$

Table 7 lists the rotor separation depending on how much the blades droop. A max of 2° droop is expected for the rotor at any flight condition. Thus, the rotor separation is set for 1.5 ft. allowing minimal exposure and reducing flat plate drag.

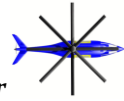
Table 7 Blade Droop Analysis

θ	H_o (ft)
1°	0.73
2°	1.5
3°	2.2
4°	2.9
5°	3.7

4.4 Airfoil Design

Optimizing an airfoil for certain conditions is an iterative process. Several methods with similar ideas exist. Each method has its advantages and disadvantages – usually a tradeoff between time and accuracy.

This airfoil optimization scheme is used for the “working” section of the rotor, or 70 to 90% of the rotor. The overall method used here was to iterate through airfoil shapes, calculating c_l , c_d , and c_m for each shape, then determining the most effective airfoil for this particular aircraft operating under certain conditions required. The baseline airfoil chosen was the VR-12, the same airfoil used for the root to 70% of the rotor.



4.4.1 Xfoil Validation

Next, an iterative scheme was designed to calculate performance characteristics of the airfoil, varying parameters angle of attack and Mach number. The iterative scheme was designed in Matlab and interfaced with Xfoil. Xfoil was chosen for its quick implementation and intense number of validations previously done. One example (among many) of a validation is show below in Figure 15.

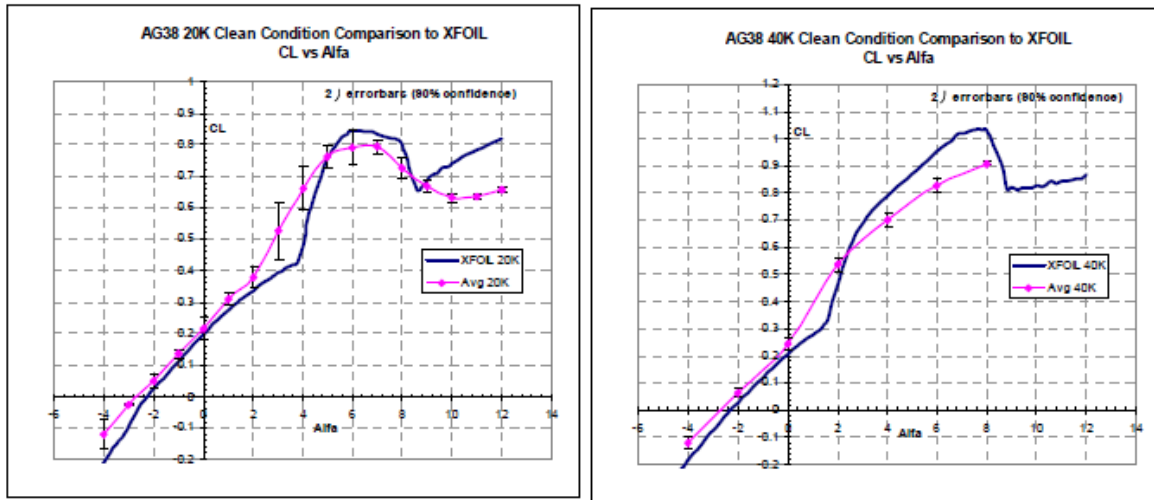


Figure 15 Validation of AG38 airfoil vs. wind tunnel data

4.4.2 Design Scheme

The next step was to define the range of angle of attacks and Mach numbers the airfoil section will encounter through all three missions. The angle of attacks were determined using a finite blade element analysis, as the airfoil section will be seeing effective angle of attacks that differ from pitch angle due to rotor inflow. This was determined to be between 2 and 5 degrees. The method to determine operating Mach numbers was to find the minimum as being the maximum forward speed minus 70% of the tip speed. The maximum was determined by 90% of the tip speed plus the maximum forward speed. Thus, Mach number ranges from 0.2 to 0.7.

With the range of operating conditions, the Matlab script iterates through 5,000 random angles of attacks and Mach numbers within these ranges, holding Reynolds number constant for each shape. Comparison of each airfoil shape is done through a Mean Standard Deviation (MSD) calculation in equation 3.

$$\frac{\sum_{i=1}^n (MSD_i)^2}{n} \quad (3)$$

The shape with the lowest MSD is the optimum airfoil shape of the shapes considered. Table 8 describes the 18 airfoil shapes iterated through.

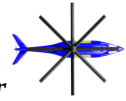


Table 8 Airfoil shapes considered for optimization

High Point	Camber	Thickness
0.2	0.01	0.09
0.2	0.01	0.1
0.2	0.01	0.11
0.2	0.02	0.09
0.2	0.02	0.1
0.2	0.02	0.11
0.2	0.03	0.09
0.2	0.03	0.1
0.2	0.03	0.11
0.3	0.01	0.09
0.3	0.01	0.1
0.3	0.01	0.11
0.3	0.02	0.09
0.3	0.02	0.1
0.3	0.02	0.11
0.3	0.03	0.09
0.3	0.03	0.1

After each shape is iterated through, an MSD is calculated for comparison between other shapes. Figure 16 shows 1/MSD on a bar graph for the 18 cases.

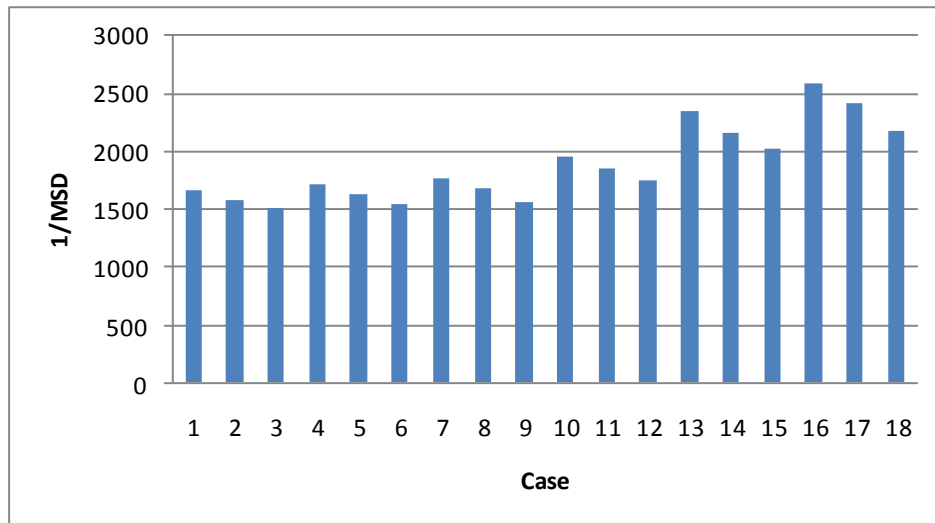
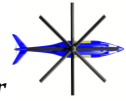


Figure 16 Comparison of 1/MSD for the airfoil shapes under consideration

Note that the 16th airfoil shape considered has a significantly higher 1/MSD and thus, the optimum shape. This relates to a slightly less thick and higher cambered airfoil compared to the VR-12 airfoil. With the 16th case considered as the optimum shape, it was then compared with the baseline VR-12.



4.4.3 DG-12

The final comparison of the two airfoils comes in the MSD, where the modified VR-12 has a value of $1/MSD$ of 2593.9 and the baseline VR-12 has a value of $1/MSD$ of 1752.1, a huge improvement of lift-to-drag ratios for the operation range of angle of attacks and mach numbers. Figure 17 shows the modified and baseline airfoil.

As discussed earlier, it is seen that the modified VR-12 is slightly less thick than the baseline VR-12. This is desired because of the location of the airfoil – towards of the tip of the rotor. Another less obvious observation is the camber – the modified VR-12 has an increased camber of 1%.

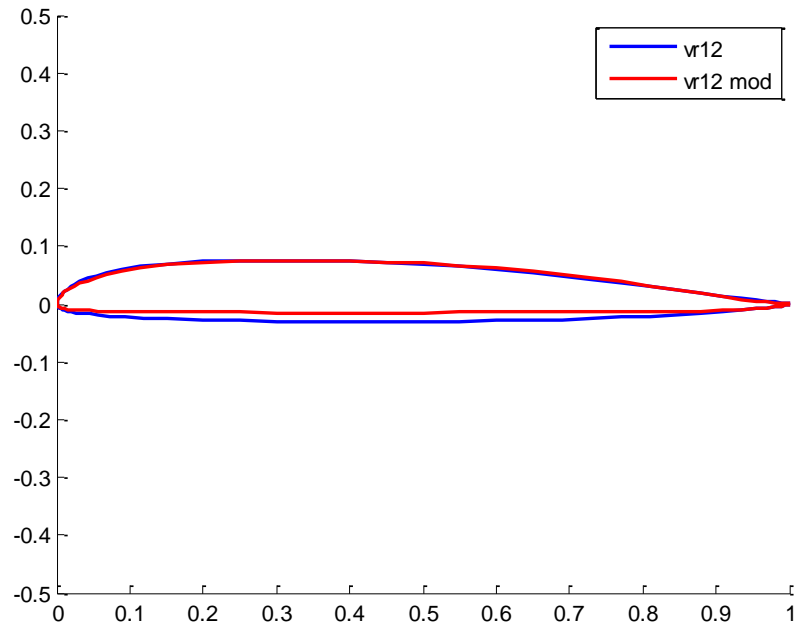


Figure 17 Modified and Baseline Airfoils

4.5 DRAG DIVERGENCE STUDY

Though the modified VR-12 was initially designed for the working section of the rotor (70 to 90%), it was also considered to work as the tip airfoil as well. However, a drag divergence study was completed to determine whether it would make for an optimum choice.

The fastest Mach number at the tip in forward flight was determined to be Mach 0.74, as shown in Figure . Therefore, utilizing Fluent with an iterative process of determining drag divergence Mach number, the ability of the modified VR-12 to serve as the tip airfoil could be determined.

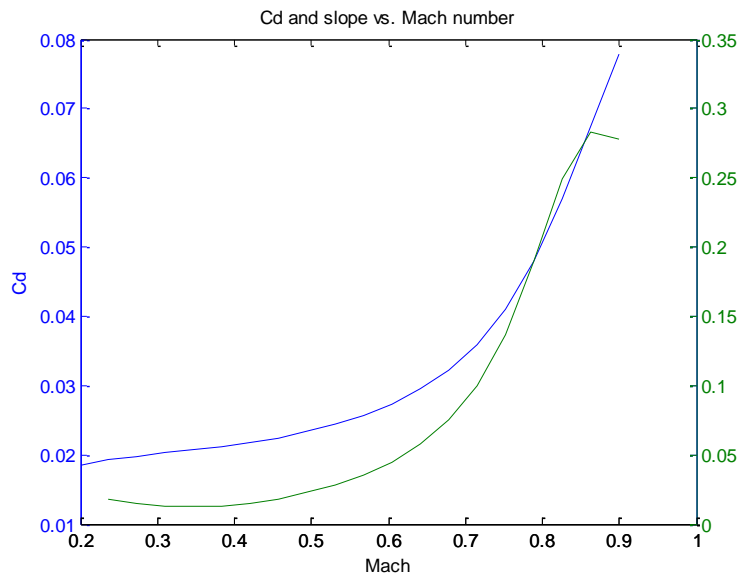
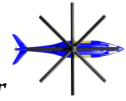


Figure 18 Drag coefficient (left) and slope (right) of drag vs. Mach number



Optimum conditions prove for the tip to be 0° angle of attack to improve lift and drag characteristics, making this the case in Fluent.

Running the case many times through Fluent at varying Mach numbers, the following graph in **Error! Reference source not found.** was obtained.

Looking at **Error! Reference source not found.**, the drag divergence Mach number is defined as the Mach number where the slope $\frac{dC_D}{dM} = 0.1$. This shows to be somewhere between Mach 0.72 and 0.73. The following series of images (Figure 20) show the reason for the spike in drag around the determined drag divergence Mach number.

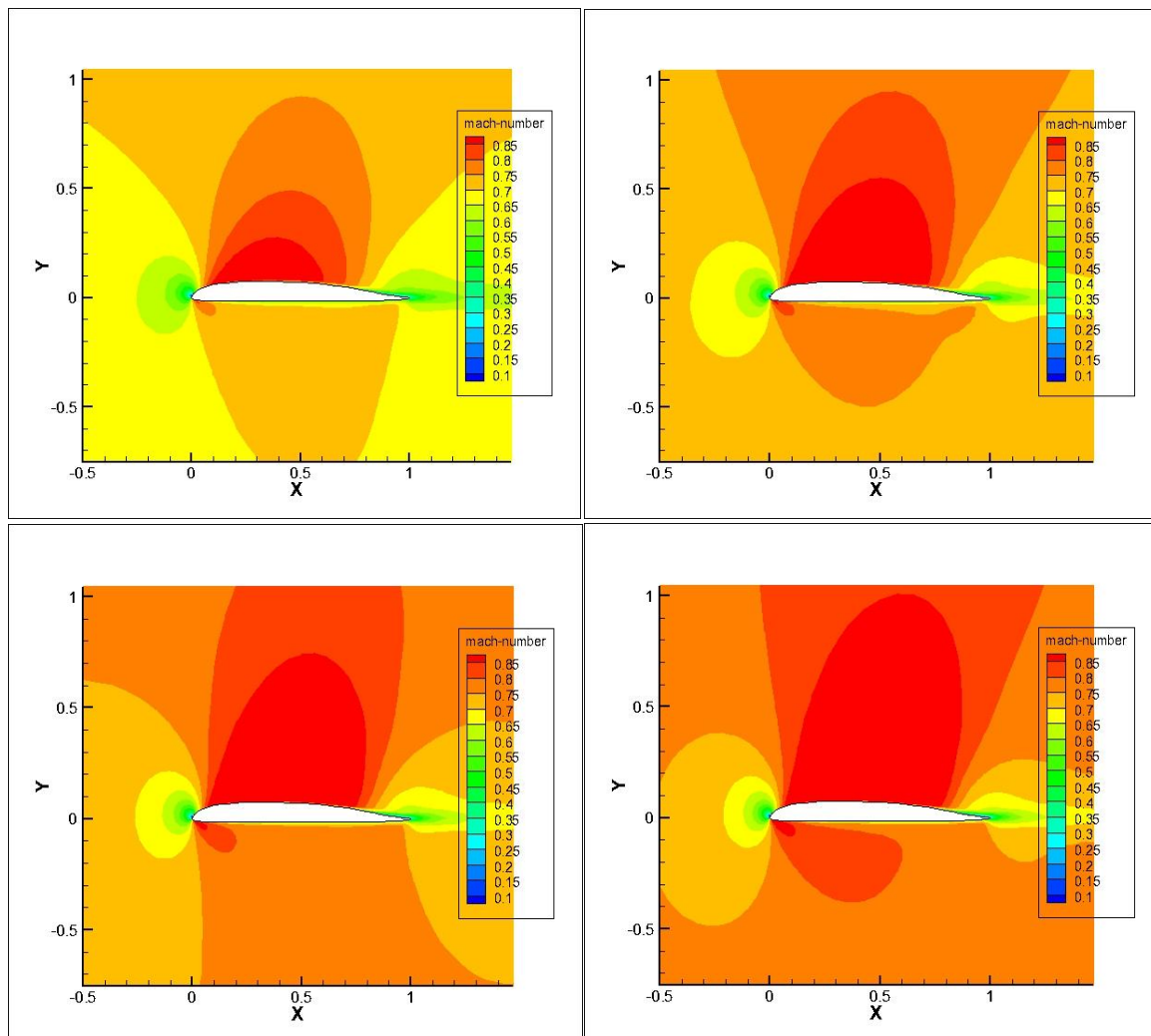
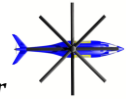


Figure 19 Series of Mach number showing drag divergence



In Figure the region between Mach 0.70 and Mach 0.74 show the formation of a shock (reaching critical Mach number). Beyond Mach 0.74, the shocks become much stronger, producing larger drag.

Because this is within a very close margin of the maximum tip speed defined above, a new airfoil must be chosen for the tip. This was chosen to be the VR-15 for its relatively thin thickness ratio and high Mach drag divergence of around 0.83 .

4.6 Final Blade Airfoil Selection

Since the working section of the rotor is critical to the performance of the rotor, the DG-12 was created for this section. The DG-12's high L/D and $C_{l_{max}}$ will perform ideally in this section of the rotor.

The baseline airfoil for the DG-12, the VR-12, will be included from the cutout to the 70% radius of the blade. The VR-12 was chosen for this section because of its high lift capability and low pitching moment. The VR-12 is excellent for maximum lift capability at lower Mach numbers typical of the retreating blade. The tip for the blade will incorporate the VR-15, purely because of its high drag divergence Mach number. Since the Golden Retriever can expect to see tip speeds of Mach 0.8 or slightly greater, the VR-15 is needed for the last 10% of the blade.

4.7 Noise Analysis

To analyze the noise created by the Golden Retriever, the Pennsylvania State University WOPWOP (PSU-WOPWOP) code was used. To create the geometry of the blade, which is an input file to PSU-WOPWOP, a Georgia Tech grid generator was used along with a converter to convert it to the proper format for PSU-WOPWOP. There are five different types of rotor noise sources, but only thickness noise was calculated for this analysis. Thickness noise is propagated in front of the rotor and is primarily generated by the geometry of the blades. In PSU-WOPWOP the microphone locations and conditions for the two main rotors and tail were inputted. **Error! Reference source not found.** confirms that all of the inputs went in properly to PSU-WOPWOP.

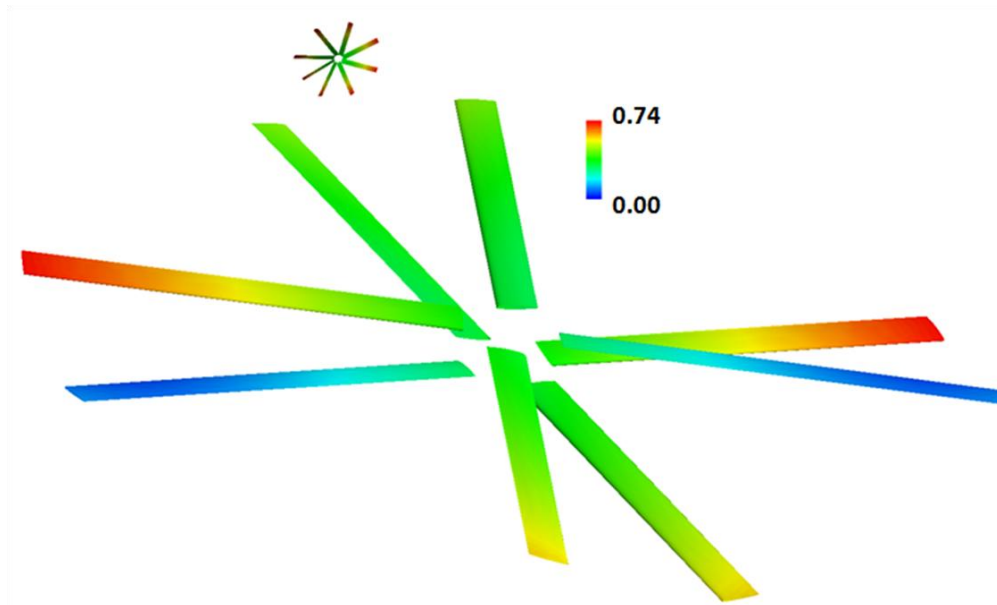
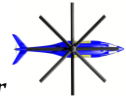


Figure 20 Main Rotors and Aux Prop inputted into PSU-WOPWOP

To view the figure the program Field View was used with the outputted sigma surfaces from PSU-WOPWOP. **Error! Reference source not found.** also confirms that the blades are spinning in the proper direction, the distance between the two rotors is correct and the placement of the tail rotor is in its desired location. The colors represent the Mach number seen on the blade. The actual Mach number can be determined from the legend. The red correlates to the advancing side of the blades that see the highest speeds.

A contour plot was generated one and half radius away from the center of the main rotor at the highest speed and tip Mach number. This was done to understand the noise around the rotor. The color represents the amplitude level of the rotor two-rotor radiuses away from the center of the rotor, see Figure . In the figure the distance to the globe wall from the center of the main rotor is one and half radius away (52 ft). It is notable that the main rotor generates far greater thickness noise then the tail rotor, particularly in front.

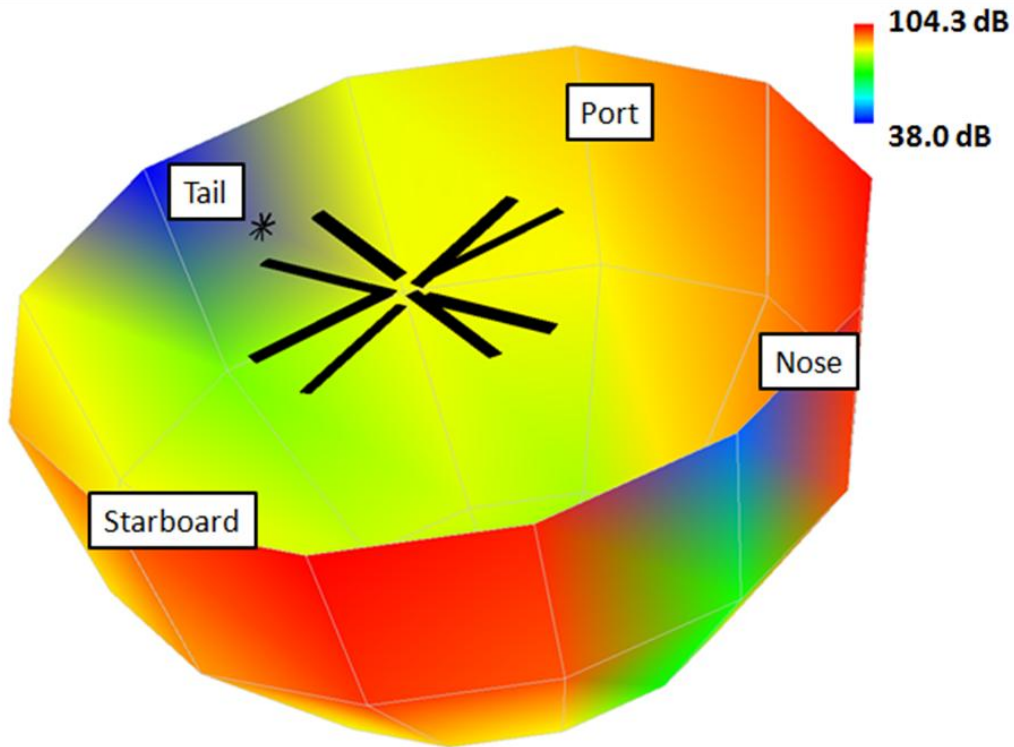
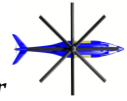


Figure 21 Two rotor radiuses away from center of main rotor

The positions runs include hover at 60 feet, forward flight at 300 feet and one mile in front of the craft. Figure 22 shows the location of the microphones. See Table 9 for the noise analysis results. For hover, the pusher prop is turned off. All of the results meet the requirements.

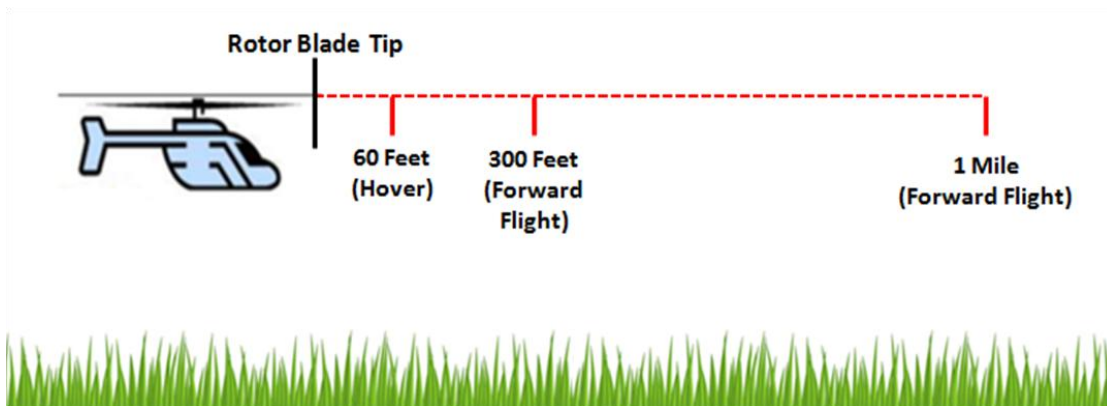


Figure 22 Location of microphones

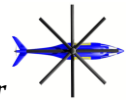


Table 9 Noise analysis results

Location Type	Location (Feet)	Requirement	Value (Thickness Only)
Hover	60 in front of rotor	85 dB	17.4 dB
Forward Flight	300 in front of rotor	90 dB	14.0 dB
In plane	1 mile in front of rotor	70 dB	0 dB

5. Fuselage Aerodynamics

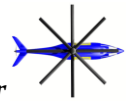
The drag on the overall aircraft was estimated using a Navier-Stokes solver from Fluent for the fuselage and estimations from the Hoerner method for the empennage and hub. The interference drag was an estimation based off the Peregrine. The estimation is based off a linear relationship between hub drag and interference drag due to hub instillation. Table 10 shows the values of equivalent flat plate drag for the fuselage, hub, and empennage of the aircraft. To put the values into perspective, Table 11 shows equivalent flat plate drag for the Lynx Mk 7.

Table 10 Equivalent flat plate drag of each component of the Golden Retriever

Component	f (ft ²)	%
Fuselage	8.25	60.99%
Main rotor hub	3.768	27.85%
Interference	1.102	8.15%
Empennage	0.40772	3.01%
TOTAL	13.52772	100.00%

Table 11 Equivalent flat plate drag of each component of the Lynx Mk 7

Component	f (ft ²)	%
Fuselage	6.31	30.02%
Main rotor hub	7.36	35.01%
Landing Gear	2.1	9.99%
Interference	1.47	6.99%
Tail rotor hub	0.84	4.00%
Empennage	0.42	2.00%
Misc. Components	2.52	11.99%
TOTAL	21.02	100.00%



The Golden Retriever has significantly less drag than the Lynx Mk 7. This is expected as the Golden Retriever should travel at much higher velocities, and thus designed to be more streamlined. The fuselage has greater drag on the Golden Retriever as it also includes the engine installation/inlets. The main rotor hub drag is significantly less, due mainly to the cover over all the linkages. This also leads to less interference drag. The empennages of both are relatively close to each other.

The Golden Retriever has a very stream lined body with retractable landing gears, reducing drag greatly. Notice in the landing gear in the Lynx Mk 7 contributes 10% of the total drag, which is completely removed on the Golden Retriever. Figure 23 shows streamlines along the fuselage of the Golden Retriever. Figure 24 shows the surface pressure coefficient contours.

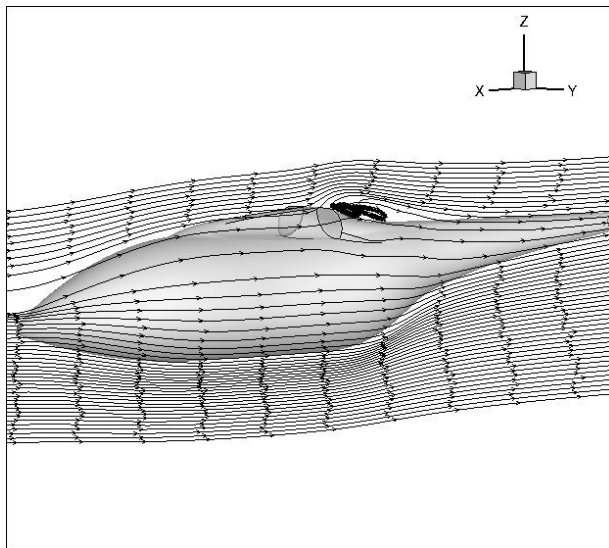


Figure 23 Streamlines around the fuselage of the Golden Retriever

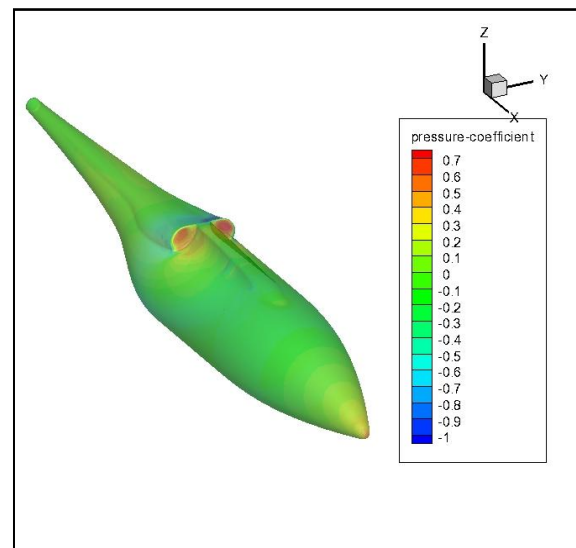


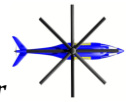
Figure 24 Surface pressure coefficient contours over the Golden Retriever fuselage

The Golden Retriever has an extremely stream lined body, except over the engine intakes. Notice the flow separation in Figure 23 just after the engine inlets. Though the abrupt change on the body causing the flow separation is expected, the effected is exaggerated due to the inlets being treated as walls. The boundary conditions are set as walls in an attempt to re-produce “ram drag”. However, this leads the streamlines around the engine exaggerating the flow separation. Therefore, the fuselage drag is a conservative estimate. The surface pressure coefficient contours re-enforce the expectations – showing a stagnation point at the engine inlets and the nose cone.

6. Yaw Control

Control of the aircraft in the z-axis in accomplished in three different ways across the three different flight regimes: Hover, Forward Flight and Autorotation. Each situation has its own concerns resulting in no one single method being effective for all situations.

6.1 Hover



In a light to mid weight helicopter, particularly one which expects to operate in hostile environments, strong yaw control authority is desired to perform critical maneuvers. Traditionally, coaxial helicopters have relied on differential collective to produce the desired yaw moment. Compared to single-rotor helicopters, the coaxial typically has less total available control moment. However, in practice it is able to achieve faster control speed because it ignores tail strength considerations.

This method of yaw control also enables the rotorcraft to complete maneuvers impossible in a single rotor helicopter.

Some concerns have been raised over the use of stiff, hingeless rotors due to their reduced flapping and therefore reduced moment capability. Nevertheless, tests have shown that this capability is reduced in a hingeless rotor by at most a factor of 2 and is easily overcome with increased collective input.

Also of concern was how large collective variance might adversely affect the performance of the rotor system. While it has been shown that best rotor efficiency is usually achieved at neutral torque condition, normal control inputs have been shown to typically increase power required by less than 7%, and only for a limited time. By considering a coaxial rotor is naturally more efficient in hover than a single rotor plus a tail rotor, in the order of over 15%, it is still a net gain that results in increased hover performance in areas like hover ceiling and vertical rate of climb.

6.2 Forward Flight

In forward flight, the rotor is unloaded and slowed, greatly reducing the effectiveness of differential control since there is very little net collective input to work off. This is not only ineffective, it is also inefficient as it produces increased drag and required profile power.

Here, the use of the tail mounted control surfaces in place of differential collective is transitioned to. Large vertical stabilizers are placed wide outside the wake of the fuselage to increase control authority. Mounted on the long arm of the tail-boom, more than adequate yaw moment from these with minimal additional drag is achieved.

6.3 Autorotation

Autorotation is the trickiest of situations for the coaxial to deal with. Reduced airspeed and change in direction of flow limit control surface effectiveness. Use of differential collective is less effective due to small net collective to work use. It is also highly undesirable as it reduces rotor energy needed to safely perform autorotational maneuvers. Additionally, since the rotor is now spinning the helicopter, yaw control inputs are reversed. As such, many different schemes of varying complexity have been developed to augment yaw control in the autorotational state. A brief survey of considered methods of supplementing yaw control is seen in Table 12.

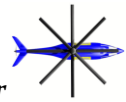
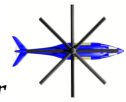


Table 12 Considered methods for supplementing yaw controls

Method	Description	Advantages	Disadvantages
Friction Braking	Mast mounted friction brakes	Simple, lightweight, large control moment achieved	Significantly reduces rotor energy
Air tip brakes or blade flaps	Tip or blade mounted air brakes create aerodynamic forces similar to differential collective	Good control moment achieved with minimal rotor energy loss.	Some reduction in rotor energy. Location makes it difficult to implement in blade design and difficult to control.
Individually Variable Transmission	Each rotor's rpm is separately controlled. Torque developed by rpm variance.	Most efficient use of rotor energy. Other control benefits in normal flight regime.	Expensive and heavy. Requires additional power to operate.

Typically in an autorotational situation generation of large moments is not necessary as most maneuvers do not require quick yaw control. And unlike a conventional helicopter, no anti-torque moment is required either, even in autorotation. Considering the above mentioned disadvantages of implementing supplemental yaw control in this situation, it was deemed unnecessary to provide additional strategies for increasing yaw control moment beyond that achieved by differential collective and tail control surface methods.

When a total engine failure occurs, the pilot will manually switch the flight control system to an autorotational mode. Control inputs will be optimized for this state and yaw control reversed to ease pilot workload. Additionally, a redundant battery powered backup for the flight control system as well as for each actuator will automatically kick in to maintain control power when electrical brown-out occurs. To conserve weight, this system will only store a limited amount of power. A reduced level of control power will be supplied during the initial stages of autorotation when only small control inputs are typically necessary. The system will always maintain enough power to allow full control authority for up to 30 seconds. This will be manually activated by the pilot prior to final approach when increased control power is required to complete landing maneuvers. Additionally, this system adds redundancy to the electrical systems as well, maintaining control power if the electrical supply is interrupted.



7. Propulsion

7.1 Engines

The CT7-8A engine was specified in the RFP; however, the engine could be rubberized to match the requirements of the design that was created. This rubberization was done by fitting a curve to engines in the CT7 family since they are designed for different power ratings. This gave the team curves comparing weight and SFC to power output. Figure 25 gives the engine weight and Figure 26 gives the SFC.

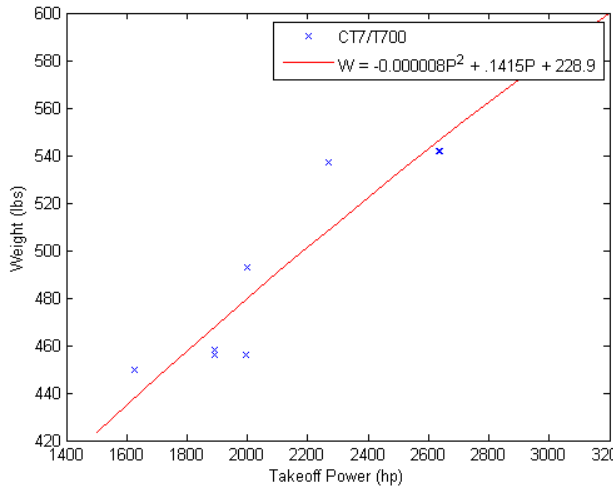


Figure 25 Weight Versus Power

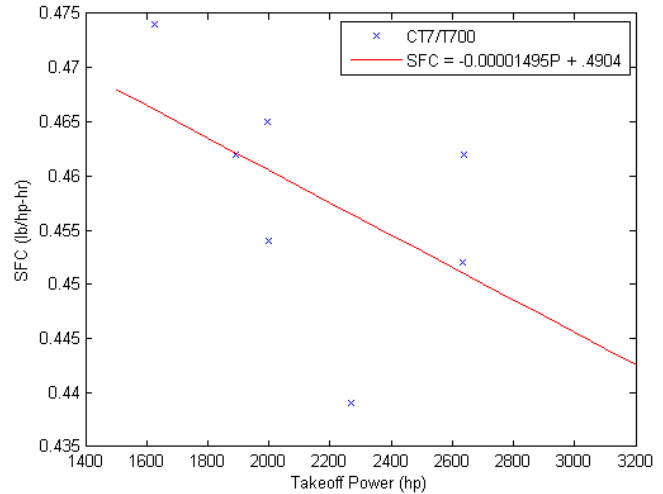


Figure 26 SFC Versus Power

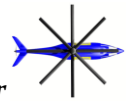
After completing the design we found that the power required was very similar to the off the shelf CT7-8A so the GE data for this engine was used. The engines were analyzed for hot and high performance using simple density and temperature ratios. Table 13 lists these parameters.

Table 13 GE-CT7-8A parameters per engine

Parameter	Value
Dry Weight	542 lbs
Sea Level Take Off Power	2634 hp
Sea Level SFC	0.452 lb/(hp-hr)
6K95 Continuous Power	2100 hp

7.2 Infrared Suppression

Infrared suppression (IR) is achieved within the airframe of the Golden Retriever. The engine exhaust is ducted to the tail boom where it is allowed to slowly mix with the cool outside air. A similar arrangement was used on the RAH-66 Comanche project and delivered a heat signature of only 25% that of a comparable helicopter without suppression. This makes it very difficult for a heat seeking missile to lock



on to the aircraft. The internal system also has the advantage of lower drag and less degradation of engine performance when compared to external IR signature reduction.

Additionally newly available active IR suppression systems can be installed on the aircraft if it is going into a very environment. These systems are very effective, but add an unneeded expense for peacetime SAR and cargo missions, so will only be carried when necessary. An example of the active IR countermeasures system is the ITT IRCM system which has currently achieved a technology readiness level of six and has been shown in tests to be effective against heat seeking munitions. The engine exhaust with its diffuser is shown in Figure 27.

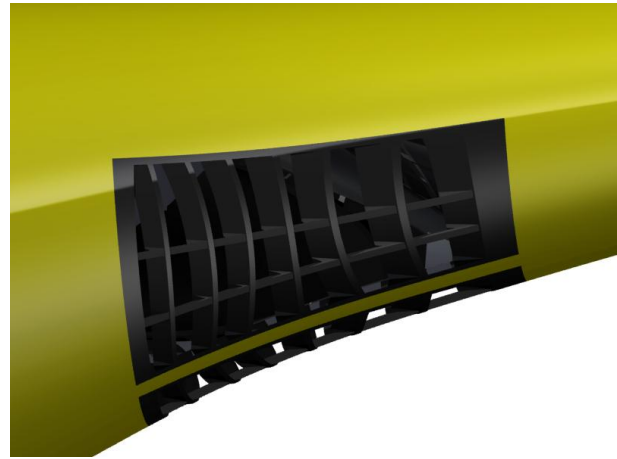


Figure 27 Exhaust

7.3 Auxiliary Propeller

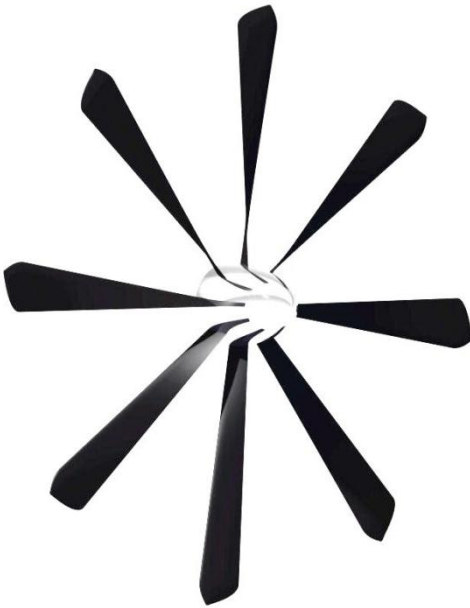


Figure 28 Aux Propeller AC2011

In high speed forward flight it is beneficial to slow the rotor to reduce the power required. It is also useful to set the rotor parallel with the direction of flight to reduce drag as well as noise. This means that forward propulsion must be produced by some other means. There are several methods of doing this. For this design three methods were considered: an internal ducted fan, jet exhaust augmentation, and a pusher propeller. Both the ducted fan and the jet exhaust solution have the advantage of no external spinning blade. This gives them an important safety advantage; however, the ducted fan is heavy and the high speed jet exhaust can kick up dust and debris. The pusher propeller has the advantage of being the lightest of the three solutions, and it allows the aircraft to operate at different pitch angles for a given airspeed because thrust can be independently controlled. Also since the pusher is not needed from low speed flight and hover a clutch and brake can be added which will immobilize it at any condition where ground personnel will be present.

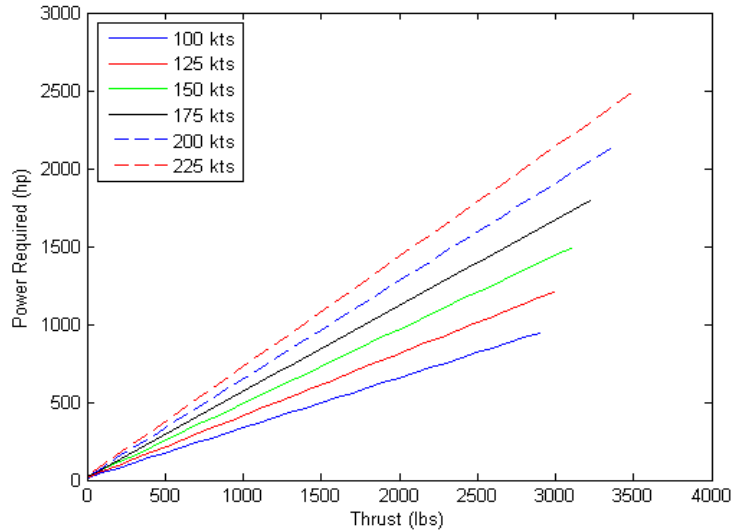
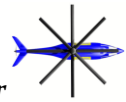


Figure 29 Power Required Versus Thrust

With the pusher propeller selected as the means of propulsion it was necessary to size it. The size was driven by the efficiency which is given by equation 4. It can be seen that the highest efficiency is when the flow is not accelerated at all and the propeller is infinitely large to give the desired mass flow. This is obviously impossible, but it shows that a larger propeller is better. In this case the geometry of the aircraft's tail limited us to a six foot diameter.

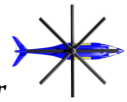
$$\eta_p = \frac{2u}{u_e + u} \quad (4)$$

Using this diameter the power needed to produce thrust was calculated using a simple blade element code created in MATLAB. This code works by summing the lift and drag forces along the blade to calculate the thrust produced and the torque needed. Torque is related to horsepower to give the requirements. This is shown in Figure 29 for various flight speeds.

Table 14 Pusher propeller parameters.

Parameter	Value
Diameter (ft)	6
# of Blades	8
Tip Velocity (ft/s)	550

The power required to overcome the vehicle drag increases with speed because the drag increases. For speeds up to 100 kts the forward thrust comes from tilting the main rotor. Thus, the power requirements for the pusher propeller are small and approximately constant in this range. Once the speed of the main rotor is decreased the pusher propeller must provide forward thrust. The power needed increases from 100 kts to the max speed of the vehicle. This is shown in Figure 30.



7.3.1 Auxiliary Propeller Thrust Scheduling

At low speeds the pusher prop is not needed, so it will be disengaged to limit the power needed to hover and perform low speed flight. As the speed is increased the drag of the propeller becomes significant if it is left in the feathered, stopped state. In the mid speed range the propeller will spin at the design speed with the blades pitched to minimize drag. During high speed flight the propeller will produce all forward thrust while the main rotor will provide only the thrust needed to overcome the vehicle's weight. The pilot will have the option to override the scheduling to allow for quick acceleration from hover, or to provide a balancing force to maintain a nose up or down attitude in hover. Table 15 lists the thrust scheduling for the aux propeller.

Table 15 Aux propeller thrust scheduling

Speed	State
0-50 kts	Propeller Stopped, Feathered
50-100 kts	Propeller Spinning, Zero Thrust
100 kts	Propeller Spinning, Forward Thrust

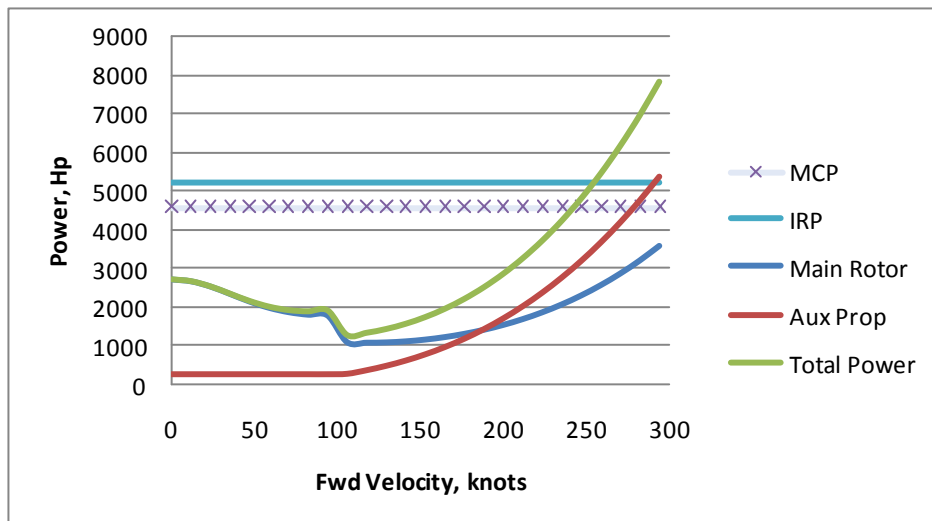
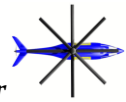


Figure 30 Aux power required vs. forward flight speed at sea level



8. Drive Train

8.1 Requirement

To design, model, and test a transmission that would take inputs from the two aircraft engines and distribute power to the main rotors and pusher prop. The main rotors must be able to operate at two different speeds, while the pusher must be able to remain stationary while the rotors are turning and engage when required.

8.2 Concept Selection

Three concepts were considered to meet the requirements:

- Two-Gear, Clutched Transmission
- Planetary Differential
- Hybrid

The simple, two gear transmission was first considered due to its simplicity. Very similar to what is found in automobiles, there would be two gears that would have to be shifted between to reach the two necessary rotor speeds. The switching from the higher tip speed to lower tip speed would be relatively simple, however, the transition from a lower to higher tip speed would be extremely difficult.

A planetary differential transmission would be able to be continuously variable, and could be electronically limited to the two necessary speeds. The configuration would involve several ‘planetary’ gears revolving around a ‘sun’ gear. This would take place inside of a ring gear that could be rotated to affect the output of the planetary gears. Either an alternative power source or power bled from the engines would have to be used to spin the ring gear in order to achieve the lower tip speed required. The extra size of this transmission compared to the simple two-speed is certainly a draw-back, however it would be much simpler to transition between the two tip speeds.

A third option would be to design a transmission that takes advantage of the best of both of the aforementioned transmissions. A continuously variable element would be implemented to shift from lower to higher tip speeds, and the transmission could simply be disengaged to slow the rotor, and then re-engaged at the proper rpm. While this may make both transitions the simplest possible, it could very well come with an enormous weight and space penalty.

8.2.1 The Concept

The planetary differential was selected based upon its ability to meet the requirements and its more off-the-shelf nature. The two engines will be meshed at a five to one ratio, reducing the RPMs from 20,000 out of the engines, to 4,000 into the planetary box. The planetary gears can then reduce the RPMs over a variable range. The output from the planetary box is then reduced at a 5.375:1 ratio through a set of bevel gears. A schematic can be seen in Figure 31.

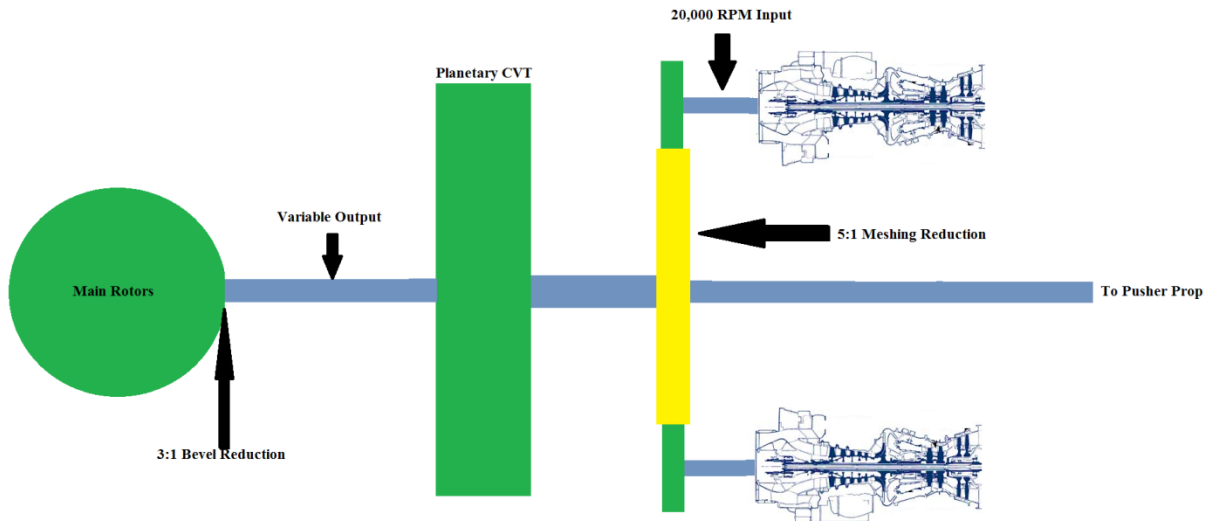
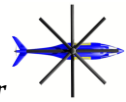


Figure 31 Drive train schematic

The meshing gears include two spur gears that take the inputs from the engines and a larger spur gear that reduces the RPM out of the engine by a factor of five. The output from this stage of the transmission comes from the larger gear in the center and is output via a shaft to the planetary gear box.

The planetary gear box consists of a sun gear, four planetary gears, and a ring gear. The sun gear takes the input from the meshing stage, operating at about 4,000 RPM. The planetary gears then rotate around the sun gear, inside the ring gear. The planetary gears are mounted on a carrier, which serves as the output from the planetary box.

The variable output of the planetary box is controlled by the rotation speed of the ring gear. When the ring gear is fixed the carrier rotates at its fastest speed, which corresponds to faster tip speeds. The ring gear is controlled via another spur gear that is powered by an auxiliary motor. That motor is capable of rotating the ring gear at 489 RPM, which then reduces the output of the planetary box to 1100 RPM.

The output from the planetary box is transferred to a set of bevel gears that complete the final RPM

reduction and transfer the power to the two main rotors. The input bevel gear outputs to two bevel gears positioned horizontally, thus rotating the rotors in opposite directions. See Figure 32 for the CAD rendering of the main rotor transmission.



Figure 32 CAD Rendering of Main Rotor Transmission

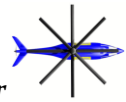


Table 16 Transmission gear specs

Gear		Weight (lbs)
System	Component	
Meshing	Input Gear (x2)	3 (6)
	Output	21
Planetary	Sun Gear	11.55
	Planetary Gear (x4)	11.55 (46.2)
	Ring Gear	102.75
Main Rotor Bevels	Input	4.47
	Output (x2)	67.8 (135.6)
Main Transmission	Rotor Total Gearing	327.57

The weight breakdown of all the gears in the main rotor transmission can be seen in Table 16. Including the shafts in the transmission, the total weight comes to 386 lbs, yielding a power-to-weight ratio of 13.472 at takeoff power. The same ratio for the Blackhawk comes to 12.430, which compares well as the Golden Retriever's transmission must operate at multiple speeds.

8.3 Stress Analysis

After the transmission was successfully modeled in AutoDesk Inventor, a stress analysis was done in AutoDesk Inventor. The simulation was run by emulating the forces applied by the two engines.

The model did not exhibit indications at any points that were susceptible to failure with any of the materials. AISI 9310 alloy steel was chosen for all gears in the system, as it is the most commonly used material in the U.S. military currently. Below in Figure 33, an example of the stress analysis can be seen with the AISI 9310 alloy being used, and the interaction between one of the input spurs and the larger meshing gear being focused on.

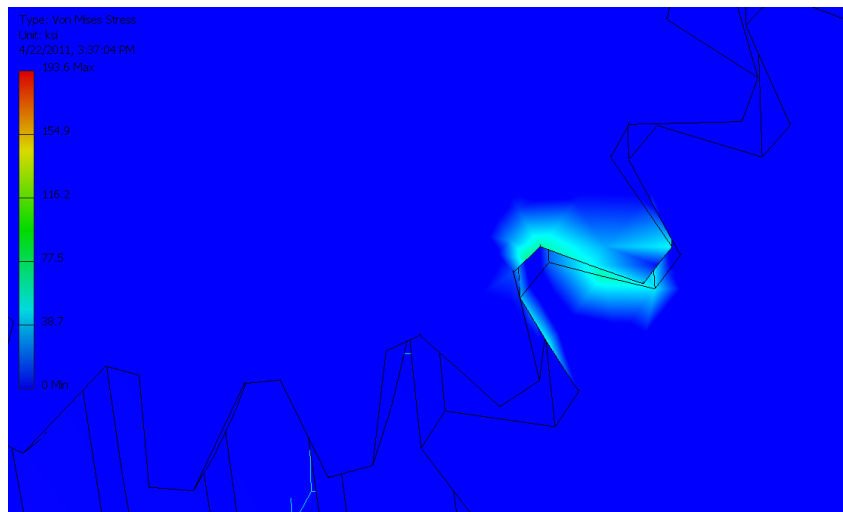
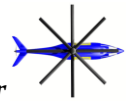


Figure 33 Transmission stress analysis



8.4 Pusher

The pusher uses the same transmission as the main rotors. A shaft from the rear of the meshing gear passes through a set of bevel gears that adjust the angle of the shaft as well as reducing it by a factor of 1.5. The shaft is then adjusted again to an angle appropriate to enter the gear box near the back of the tail via a universal joint. The shaft then enters the pusher gear box that further reduces the RPMs by a factor of 1.16, which yields the desired tip speed of 720 ft/s.

Also included in the pusher gear box are a brake and a clutch that allows the pusher to rotate freely when the transmission is not engaged. When the pusher is desired the clutch engages and the pusher operates at the design conditions.

9. Structures

9.1 Requirements

In order to show that the structural design of the Golden Retriever can satisfy the specified mission, the following structural requirements must be met: low empty weight fraction (~18,000 GTOW), 2-door deployment capability, M/R load analysis, auxiliary propulsion load analysis, mission-specific load analysis, 1 degree blade stiffness to minimize droop, and an airframe capable of withstanding pull-up loads of up to 3G's. After identifying the structural requirements, material selection for each part was conducted.

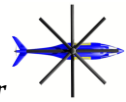
9.2 Material Selection

In choosing the material breakdown for the Golden Retriever, it is important to consider cost, weight, manufacturing, part count, durability, resistance to corrosion, and fatigue life. For these reasons, composites were chosen as the prime material, accounting for at least 80% of the material configuration on this helicopter. Notable aircraft companies, namely Bell Helicopter, Sikorsky, and Boeing, have used a large percentage of composites in their current helicopter designs. *Helicopter Composite Materials Applications*, a technical paper written by representatives of the three aforementioned companies, attest to the benefits of composites. After deciding to use composites, questions then turned to which type of composite to use for each structural component, methods of bonding, satisfaction of material and mission requirements, and obtaining a stress/load analysis of the helicopter with the material specifications. These questions resulted in numerous trade studies, material property specifications, and concluded in a finite element analysis.

9.2.1 Trade Study

Trade Study Conclusions

From various sources mentioned in the reference section a conclusion of the best material was made. Based on the results of the composites versus metal trade study, the Golden Retriever incorporates a majority-composite airframe made of a graphite/epoxy and Nomex sandwich construction for larger components and carbon skin for smaller parts. The main benefits of composites are weight reduction, high



strength-to-stiffness ratio, low corrosion, and reduction of parts. While the anisotropic nature of composites is not conducive to mass production of this helicopter, it enables tailoring for an optimal configuration of the Golden Retriever to achieve mission requirements. Reductions in cost can still be seen when incorporating the reduction in metal parts and long-term maintenance/labor costs. Detailed material properties and the breakdown of each component that makes up the Golden Retriever will be further described in the following sections.

9.2.2. Material Properties

After the trade study was conducted, the use of T300/976 graphite/epoxy was deemed most appropriate to meet FAR/mission requirements. Table 17 lists the properties of a high-modulus carbon/epoxy lamina.

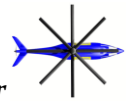
Table 17 T300/976 Graphite/epoxy properties

Property	Value
Longitudinal Young's Modulus	$1.25 \cdot 10^{11} \text{ N/m}^2$
Transverse Young Modulus	$8.45 \cdot 10^9 \text{ N/m}^2$
Shear Modulus in XY Plane	$4.3 \cdot 10^9 \text{ N/m}^2$
Shear Modulus in YZ Plane	$2.45 \cdot 10^9 \text{ N/m}^2$
Poisson's ratio	.318
Density	1550 kg/m^3
Shear Stress Limit in XY Plane	$7.653 \cdot 10^6 \text{ N/m}^2$

Table 18 Nomex Honeycomb core properties

Property	Value
Young's Modulus in X Plane (E_{11})	$8.04 \cdot 10^6 \text{ N/m}^2$
Shear Modulus in YZ Plane (G_{23})	$7.58 \cdot 10^{10} \text{ N/m}^2$
Shear Modulus in XZ Plane (G_{13})	$1.206 \cdot 10^7 \text{ N/m}^2$
Shear Modulus in XY Plane (G_{12})	$3.22 \cdot 10^7 \text{ N/m}^2$
Poisson's Ratio	.25
Density	48.1 kg/m^3
Shear Strength	$8.605 \cdot 10^5 \text{ N/m}^2$

Additional material considerations were based on protecting the helicopter from electromagnetic attack, particularly through the windows. Laser systems not only remotely attack an enemy, but the rays alone can be eye damaging. Incorporating layers of metallo-dielectric material on the windows maintain its transparency will protect against EMI and IR waves.



9.3 Coax Structural Layout

Concept

The layout of the Golden Retriever's structural configuration is similar to the Sikorsky S-97 Raider, a helicopter in production stemming from X2 technology. Its development is projected for 2014. With its purpose as a high-speed military helicopter, the structure reflects aerodynamic considerations not usually seen on a helicopter. Aurora, a company based in Virginia, won the contract to design and fabricate the S-97 airframe. To meet their goals for speed, lightweight composites were used in conjunction with the coaxial rotor, pusher, and H-tail.

9.3.1 Description of What Coax Includes

The Golden Retriever model emulates the sleek configuration of the Raider, H-tail, and composite use. Below is a breakdown of the airframe by part. The forward fuselage consists of the nose, cockpit, and cabin. The aft fuselage contains the tailboom, horizontal, and vertical stabilizers, see Figure 34. The structure is kept intact by the addition of longerons, bulkheads, stringers and ribs to maintain the strength and form of the helicopter.

Table 4.4.5 from *the Department of Defense Composite Materials Handbook* details the criticality of structural components in a helicopter configuration. Based on the criteria, the primary parts needed are the tailboom, pylon support, frames, longerons, ribs, spars and skins. These components are necessary in all rotorcraft configurations as internal and external load-bearing structures. The flight critical secondary components are the cabin doors to transport people and cargo during the mission. The placement of these primary and secondary components is further described in Section 9.1.2.

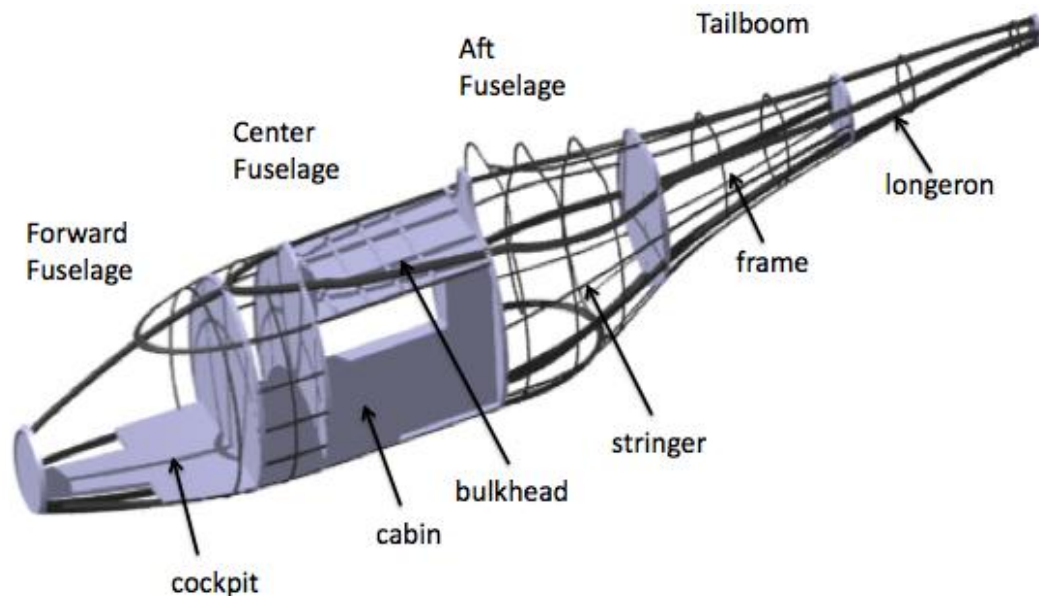
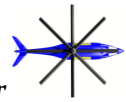


Figure 34 Primary Structural Breakdown

9.3.2 Placement Of Parts And Reasoning

After determining the necessary parts to maintain the structural integrity of the Golden Retriever, the placement was determined based on important load-bearing locations. This helicopter contains longerons



that span from the nose to tail at the base of the helicopter, and at the helicopter ceiling. There bulkheads connecting the upper and lower longerons, located in the front and aft portions of the cabin and along the tailboom. Stringers have been evenly distributed between the longerons and frames between the bulkheads and are placed where concentrated loads are applied.

9.4 Structural Breakdown

9.4.1 Forward Fuselage

The forward fuselage consists of the nose and cockpit. The panels consist of a sandwich structure of graphite/epoxy and Nomex honeycomb. The Nomex component consists of 48 plies of .13 mm with a core thickness of 5cm and (0/+45/90) layup. T300/976 graphite/epoxy in a (0/+45/90) layup with surrounds the Nomex. The windows will incorporate a metallo-dielectric material, as previously mentioned, which is used to improve helicopter and crew survivability against hostile electromagnetic waves. Further material considerations for pilot safety in the cockpit will be discussed in section 9.5 (Crashworthiness/Fatigue).

9.4.2 Center Fuselage

The center fuselage consists of the cabin and sliding doors. The cabin has been designed to provide enough space necessary for the missions, particularly the search and rescue mission. The floor has fasteners designed for reconfigurable layouts of the cabin according to arrangements needed for varying payload and to transport injured passengers is needed. The panel structure will be the same as that of the forward fuselage, but with a greater thickness to accommodate for the larger dimensions.

9.4.3 Aft Fuselage

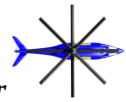
The aft fuselage is made up of the tailboom and vertical stabilizer. The tailboom structure for the panels is again like that of the forward and center fuselage. The “H-tail” vertical stabilizer configuration was chosen to reduce drag effects and delay the onset of divergence at higher speeds. It enables the helicopter to maintain steady motion in forward flight during the missions. The S-97 raider uses an H-tail for the same reason, and anticipates breaking the X2 speed record despite its larger size and weight. (The X2 vertical stabilizer uses fins in the $-z$ direction).

9.4.4 Additional Parts

The longerons, stringers, bulkheads, spars, and frames of the Golden Retriever consist entirely of 1 in thick carbon skin. By using stiffer type of carbon skin, the frame remains sturdy, light, and has a stress to strain tolerance.

9.5 Crashworthiness/Fatigue

A very important aspect to consider in defining the Golden Retriever structure is its crashworthiness. Crashworthiness is defined as the ability of an aircraft and its internal systems and components to protect occupants from injury in the event of a crash. The strength of the helicopter through the structure/materials chosen is integral in the helicopter’s lifetime, passenger safety, and performance under extraneous conditions. According to a number of epidemiological studies, up to 90% of crashes could be



survivable (Haley and Hicks, 1975; Hicks, Adams, and Shanahan, 1982; Shanahan and Shanahan, 1989). In the past, the airframe and its parts have not been considered as a means of ensuring vehicle safety and protection, but ongoing research has begun utilizing these components for that purpose.

An acronym known as CREEP (**C**ontainer, **R**estraint, **E**nergy absorption, **E**nvironment, and **P**ostcrash factors) summarizes the basic principles of crashworthy design. These concepts will be explored followed by current structural technology solutions for crashworthiness. Finally, adaptations made for the Golden Retriever Layout will be addressed.

Container

The container, or cockpit and cabin, should have enough strength to protect the occupants by incorporating a protective shell in the fuselage design. The belly and nose of the helicopter should be shaped to prevent plowing of earth during high-velocity crashes. The design should allow for a maximum of 15% deformation upon crash to increase chances of passenger survivability.

Restraint

Restraint includes the seats, restraints, systems and their attachments; they should have enough strength to keep occupants in place when subject to large loading. Seat attachments should also be able to withstand significant warpage without failure. In most helicopters, both lap belt and torso restraint are necessary for crash survivability. A tie-down strap is another form of restraint that prevents submarining, when the lap belt compresses soft organs of the abdomen.

Energy Absorption

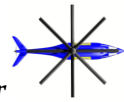
Most helicopters are not equipped with crushable material that can properly absorb impacts. Three main areas that help with absorption are in the landing gear, floor structure, and seats. The landing gear, if extended, can handle up to 50% of crash impact, but if retractable landing gear is used, more emphasis should be placed on the structure and seats. Energy-absorbing seats have become effective in preventing injuries, especially those that provide purely vertical stroking. The average load level should not exceed 14-15G for military helicopters.

Environment

It is necessary to consider the internal environment surrounding an occupant when seated in a helicopter. There should be no sharp or dangerous objects within the radius of human occupation during dynamic crash conditions, also referred to as the strike zone. Using upper torso restraints is especially important to protect vital organs.

Postcrash factors

Hazards to consider upon crashing include proximity to fire, fumes, oil, and water. Options for human safety include means of preventing or controlling the hazard; if that cannot occur, escape routes should be explored. Methods to promote safety include crash resistant fuel systems, the use of fire resistant/low toxicity materials in aircraft construction, and to separate flammable materials from ignition sources. When considering crashes in water, helicopter flotation devices, emergency lighting/exits, and personal underwater breathing devices should be incorporated in helicopter configurations.



Structural Considerations from CREEP

The Golden retriever has incorporated a number of mechanisms in its design to maintain crashworthy standard. They include the incorporation of composites, which are resistant to high temperatures. The Nomex honeycomb core is not only lightweight, but the honeycomb structure is crushable and is useful in absorbing impacts. Seats with strong attachments to prevent warping and tie-down restraints to contain the lap and upper torso are equipped in the cabin and cockpit. An isolated, crash-resistant fuel system is used to prevent the onset of fires upon impact. The aerodynamic shape of the nose and belly of the Golden Retriever prevents scooping and plowing of earth when a crash occurs, to protect a passenger from the backlash of an abrupt reduction in velocity.

9.6. FINITE ELEMENT ANALYSIS

The final step in assessing the structural integrity of the Golden Retriever was through a stress analysis using CATIA and ABAQUS. The airframe model was first uploaded in CATIA and meshed to analyze the effects of a distributed load at various key points along the configuration. Material parameters were then defined by using the values listed previously. Parts were specified based on the structural breakdown, incorporating the graphite/epoxy skin for the longerons, bulkheads, stringers, and frame and using a Nomex-graphite/epoxy sandwich structure for the remainder of the helicopter

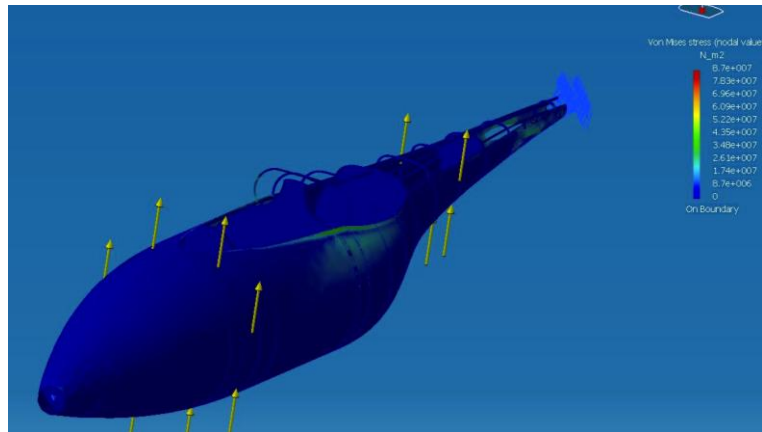


Figure 35 Finite Element Model

airframe. Figure 35 shows a stress analysis conducted in CATIA. After creating a mesh, identifying the material, and specifying an applied distributed load, a structural analysis could be conducted. The colorbar on the right represents the Von Mises stresses, which can be compared to the material's own strength to determine if it can handle the force applied. In this case, the force was 34,000 N, or twice the weight of the helicopter, which it was able to easily withstand. The blue shading on the helicopter represents low Von Mises stresses on the body.

Due to the complexity and anisotropic nature of the specified composites and the current license of CATIA available to Georgia Tech students, the material parameters could not be processed in CATIA. As a result, the mesh and components of the Golden Retriever were imported into ABAQUS, which has more capabilities in processing user-defined materials. A drop test was performed and the results were exported into a set of stress-strain graphs. These results were compared to the known maximum strength values for graphite/epoxy and Nomex core. CATIA was still used to analyze the results for a metal baseline by using a material defined in the software. With both sets of models, an approximate percentage weight reduction could be seen as well as key load-bearing components and the strength of the materials under stress.

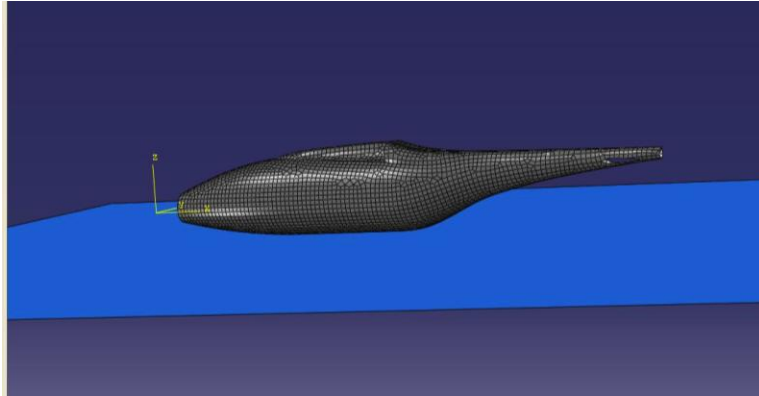
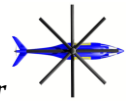
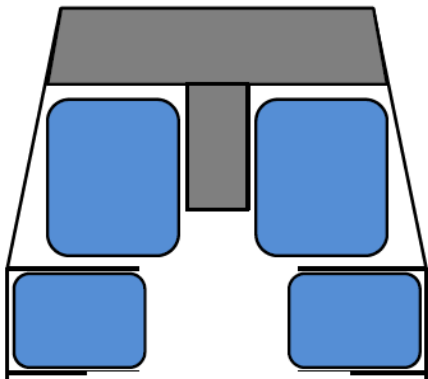


Figure 36 ABAQUS drop test layout

Figure 36 is the setup of the drop test in ABAQUS as it is running. In order to expedite the running time, an artificial floor (in blue) was created and the helicopter was dropped at a high velocity to simulate the impact of falling at a higher height. A drop test is a good preliminary test of the material strength of a helicopter, but further useful analyses should be made to simulate crashworthiness and analyze lift at hover and forward flight.

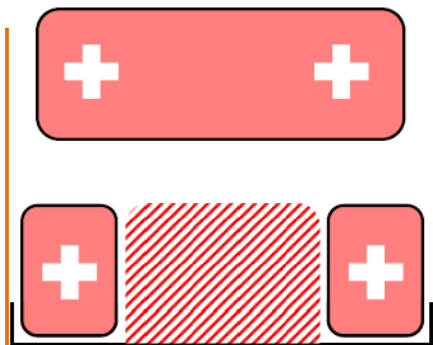
10. Reconfigurable Cabin

Since the Retriever is designed as a multi-mission aircraft, cabin configuration is an important part of the design. All three primary missions require different types of configurations to meet their different payload needs. Additionally, it is important that the cabin be quickly reconfigurable to allow the vehicle to change roles in the field with minimal effort and limited equipment. To achieve this, the Retriever features a system of hard points along the interior of the cabin to which modular equipment such as seats or stretchers are attached depending on the mission.



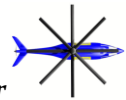
Mission 1

For the search and rescue mission space and access considerations are critical. In the center of the cabin is the stretcher tower. A flexible frame is attached to floor and ceiling hard points. This frame is designed to accommodate two standard stretchers with dimensions up to 86"x27" and weight of 350 lbs. each. Stretchers are then stacked in the tower one above the other. This gives each patient over 36" of headroom, allowing medical personnel easy access. Due to landing site hazards or urgent medical needs, quick loading/unloading is essential. Designed to accommodate a variety of stretchers, already loaded litters can be quickly slid into the frame instead of having to transfer patients from one stretcher to another. If the patient is not already on a litter, onboard litters can be removed allowing personnel to put them on a litter outside and then reinsert the litter in the frame. This saves time over having to maneuver an injured patient into the helicopter and onto a statically mounted bed. Additionally, the litter's perpendicular orientation allows the litters to be accessed easily by all 4 crew members.



- Mission 1: Search and Rescue**
- 4 Crew
 - 2 Medical Personnel
 - 2 Occupied Litters
 - 500 lbs. Medical Equipment

Figure 37 Mission 1 Layout



for 2 medical personnel are located in the rear of the cabin. These seats are 18” wide and can accommodate up to 350 lbs each. Between them is an open cargo area designed to provide the medical personnel easy access to medical supplies and equipment. Medical equipment in containers can be lashed to the deck using mounting points or stowed in a larger container that mounts to the cabin wall.

Mission 2

In a personnel carrying capacity, the Retriever has ample room to carry 6 passengers. Hanging seats similar to those used in the other missions can be attached to hard points quickly. The flexible structure of the seats not only allows for easy attachment/detachment but also means the lightweight seats can be folded and stowed easily and compactly. Since this is true for components from other missions as well, it is possible to carry spare components options, giving the Retriever true multi-mission capability in the field. One example might be an outbound leg with troop carrying capability similar to Mission 2, followed by a quick switch to a medevac role similar to Mission 1 to carry injured troops on the return leg.

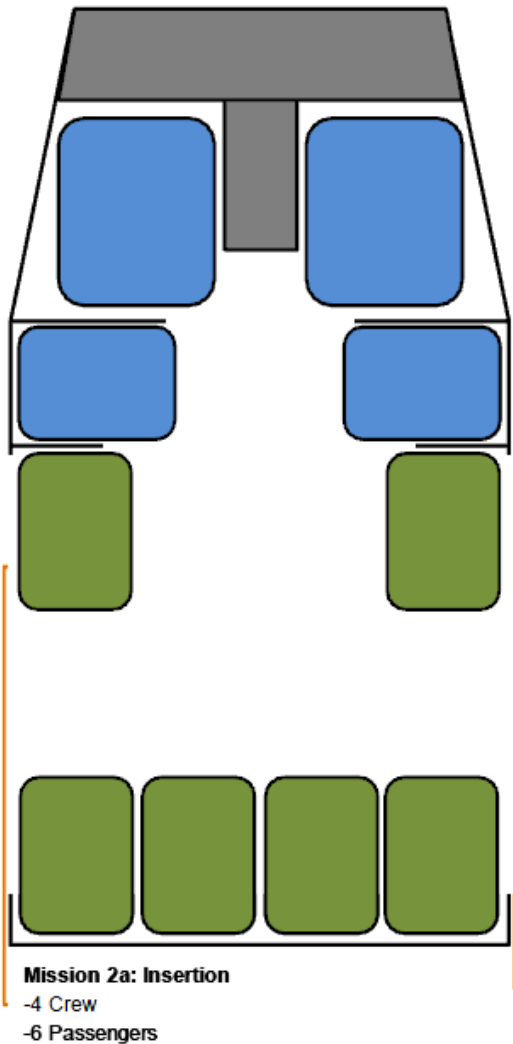


Figure 38 Mission 2 configuration option a

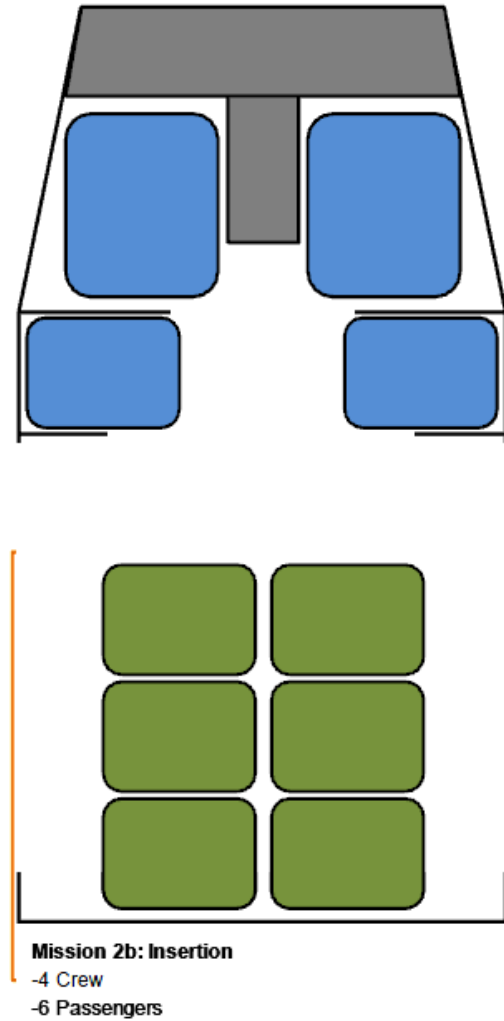
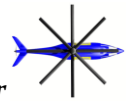


Figure 39 Mission 2 configuration b



All seats and litters are equipped with load limiting devices to reduce shock loading in a crash situation. Consisting of specially sewn webbing designed to rip only under high loads, these stitch ripping devices (SRDs) have a very high specific energy absorption (22-30 J/g)¹ with limited total extension compared to other load limiting devices. This makes them a lightweight, unobtrusive way to increase the crashworthiness of the aircraft.

Mission 3

With an array of hard points on the ceiling and bulkheads, securing loads, such as those in Mission 3, is very simple. Irregularly shaped loads can be lashed to the deck or placed in containers specifically designed to mate with the hard points. And with a large cargo area the crew will have more options when it comes to arranging the load and balancing the aircraft.

Designed to be study but simple, the cabin systems of the Retriever are designed to be safe and light weight, reducing empty weight and increasing payload capability. They are also quick and easy to configure: and experienced crew should be able to completely change configurations in 10 minutes or less without additional equipment. Moreover, strategic placement of the points allows additional configurations beyond what is shown here. Some examples might include a triage configuration where two stretcher towers are used in lieu of the medical crew. Or a deep evacuation mission where auxiliary tanks are fitted to extend the range of the Retriever, then jettisoned and replaced with seats for the return leg. Auxiliary tanks could also be used in a ferry situation allowing the Retriever to be self-deployable.

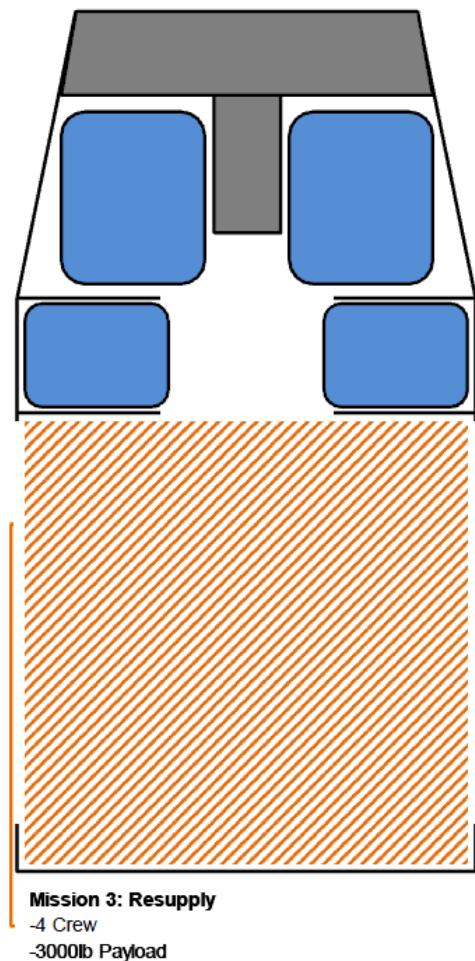
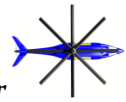


Figure 40 Mission 3 Configuration

11. Vehicle Performance Calculations

11.1 Power Required

The power required of the vehicle was calculated using simple momentum theory with correction factors. This analysis was done in Excel. The power required calculation is made up of the profile power and induced power of the rotors, and the parasite power of the vehicle. The model created in Excel was first



validated with existing production rotorcraft. Figure 41 plots the power required vs. power available of the Sikorsky UH-60 and X2. Data for these helicopters were widely available which is why they were chosen for the validation. The max speed for the UH-60 is approximately 160 knots which agrees very well with the Excel spreadsheet.

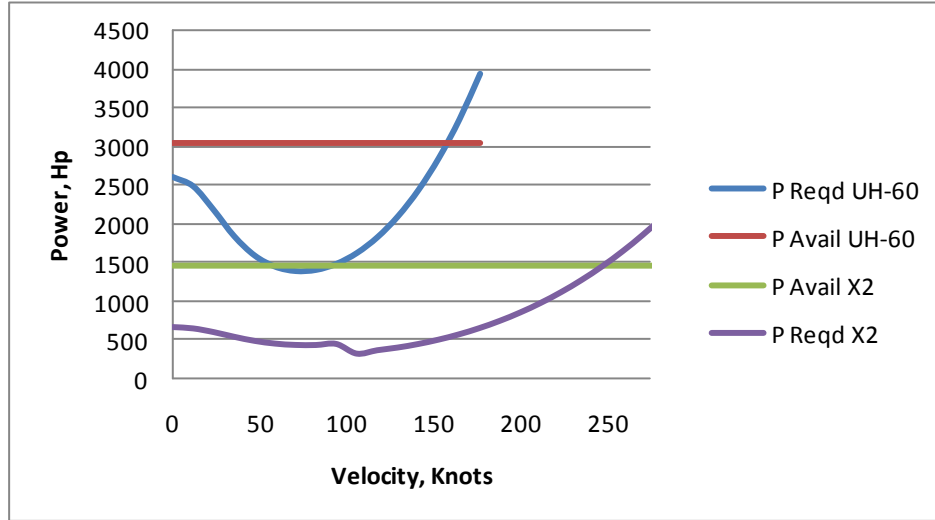


Figure 41 Validation of power required code

The power required of the Golden Retriever could now be calculated. Equations 5 and 6 were derived in order to accurately calculate the induced and profile power of the coaxial rotors.

$$P_{i_{Total}} = P_{i_{upper}} + P_{i_{lower}} = \frac{\left(\frac{W}{2}\right)^{3/2}}{\sqrt{2\rho A}} + \frac{\left(\frac{W}{2}\right)^{3/2}}{\sqrt{2\rho A}} = \frac{2\left(\frac{W}{2}\right)\left(\frac{W}{2}\right)^{1/2}}{\sqrt{2\rho A}} = \frac{W^{3/2}}{\sqrt{4\rho A}} \quad (5)$$

$$P_{o_{Total}} = P_{o_{upper}} + P_{o_{lower}} = \frac{\rho A V_T^3 \sigma C_{do}}{8} + \frac{\rho A V_T^3 \sigma C_{do}}{8} = \frac{\rho A_b V_T^3 C_{do}}{4} \quad (6)$$

For the performance of the Golden Retriever, the profile power experiences a drastic change at 100 knots. This is due to the tip speed reduction from 650 ft/s to 450 ft/s. This is very beneficial from a power required standpoint since the profile power is a function of the cube of the tip speed. Figure _ plots the power required vs. the power available along with the induced power, profile power, and parasite power at sea level. These calculations were also made at 6K95 and those results are plotted in Figure 42 and 43.

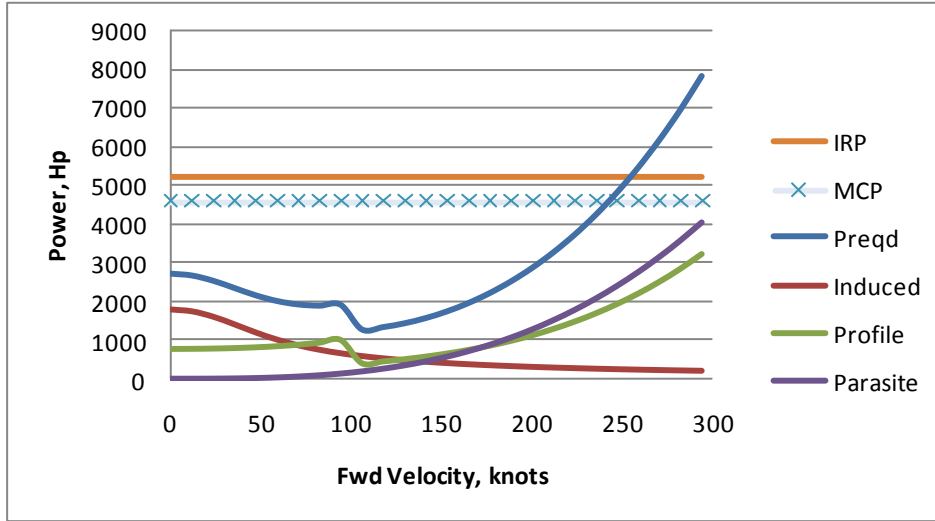
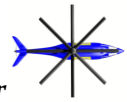


Figure 42 Power required at sea level

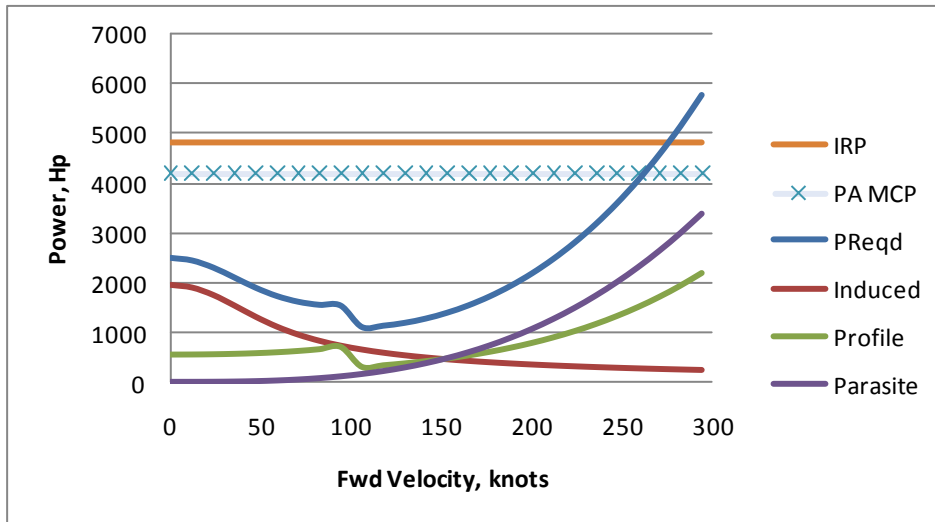
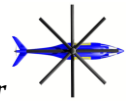


Figure 43 Power required at 6K95

It is important to note that even at 6K95, the Golden Retriever has a nice power cushion to hover and it can well exceed the 225 knots minimum for the medevac mission.



12. Weight Analysis

The CIRADS sizing discussed in section 3.3 yielded a weight breakdown, which provided a guideline for the weight analysis. The CIRADS breakdown can be seen in Figure 44.

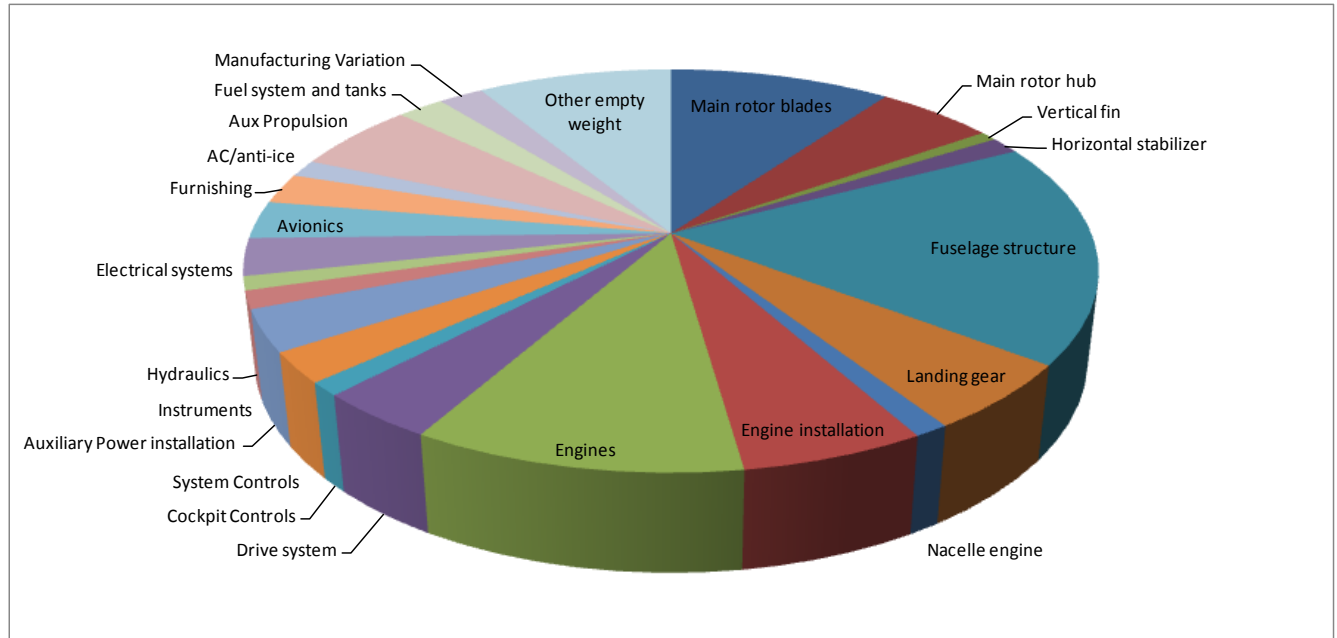


Figure 44 CIRADS Weight Breakdown

Weight Estimation

An initial weight estimation using equations that utilize a trend analysis to determine the weights of component groups was done. Avionics weights are based on the sum of the weights of the individual instruments and systems needed to operate the helicopter. Further analysis through CIRADS and CATIA gave more accurate weight results for sized components such as the rotor and airframe groups. The weight build up can be seen in Table 19, where the accuracy of the model is within 4% error. The pie chart in Figure 45 shows a percentage breakdown for the heaviest mission set, insertion.

Center of Gravity

Through analysis of all three missions the CG of the vehicle was found to lay, with default fuel settings, a maximum of 2 feet ahead of the rotor shaft. This, however, will not affect the performance of the vehicle as it has incorporated a system of fuel pumps to move fuel into rearward compartments; thereby, moving the CG back towards the rotor shaft. For this maximum CG condition, the fuel compartmenting system, with maximum available rearward space can move the CG at most -1.6' bringing the CG location to approximately 6" forward of the rotor which can easily be compensated for by the rotor controls.

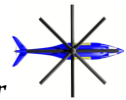


Table 19 Weight Buildup

Parts	Weights (lb)			
	Mission:	Medevac	Insertion	Resupply
Rotor/Hub	1518	1518	1518	1518
Blades	991	991	991	991
Hub	527	527	527	527
Propulsion/Fuel	3540.9	4134	4090	4090
Fuel Systems	151	151	151	151
Engines	525	525	525	525
Aux prop	280	280	280	280
Drive system	400	400	400	400
Fuel	1,768	2361	2317	2317
Oil	32	32	32	32
Transmission	385	385	385	385
Avionics	772.5	772.5	772.5	772.5
Installation	40.2	40.2	40.2	40.2
Communication	170.3	170.3	170.3	170.3
Navigation	156.5	156.5	156.5	156.5
Controls and Displays	299.6	299.6	299.6	299.6
Survivability Equip	105.8	105.8	105.8	105.8
Payload	2254	6040	3840	3840
Passengers	400	1200	0	0
Litters (occupied)	514	0	0	0
Equipment	500	4000	3000	3000
Crew	840	840	840	840
Airframe	5226	5264	5150	5150
Passenger Seats	76	114	0	0
Fuselage	4367	4367	4367	4367
Fuel Cells	150	150	150	150
Hardware	100	100	100	100
Landing Gear	333	333	333	333
Crew Seats	200	200	200	200
Total	13312	17729	15371	15371
Empty	11058	11689	11531	11531

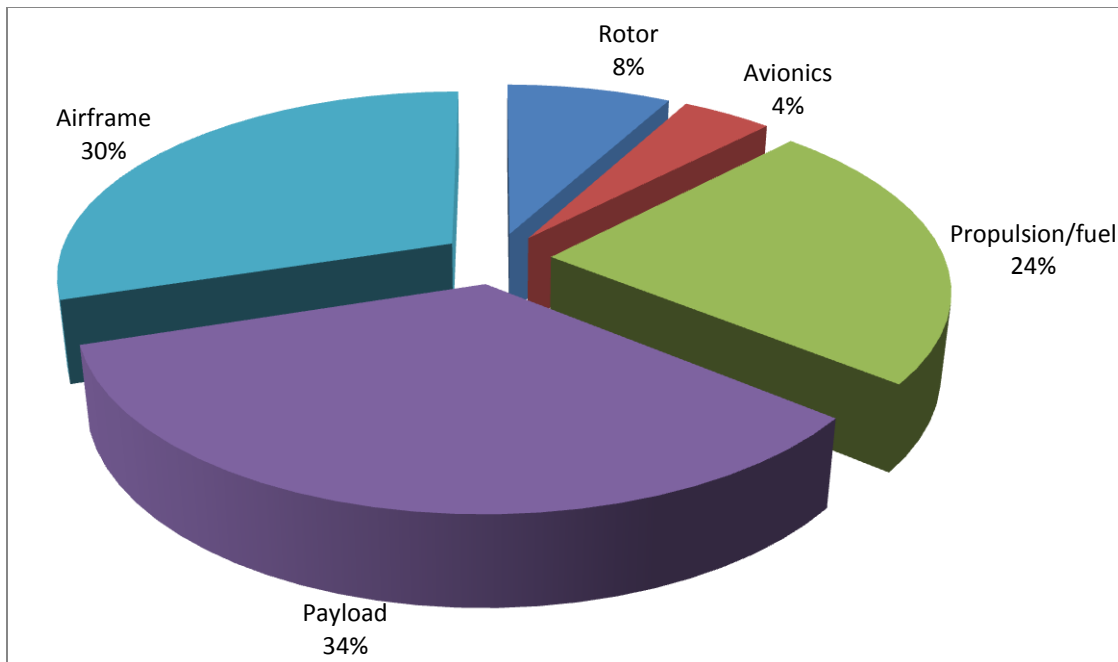
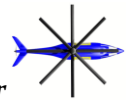


Figure 45 Insertion Mission Weight Percentages

13. Cockpit And Cabin Systems

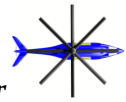
In order to eliminate the vibrations throughout the cabin, active vibration control systems will be placed in the cabin. These systems will be similar to those currently found in the Bell 429.

The cockpit and cabin systems consists of 4 crew seats, Avionics installations, communications gear, navigation software and hardware, Aircraft survivability equipment, controls and display systems, and safety equipment.

The avionics installation framework is made almost entirely of composites, increasing the strength of the fit to the airframe while also increasing the cockpit space available for crew movement or additional supplies

The communications gear includes a Raytheon AN/APX-100 IFF transponder it is the smallest fully integrated military transponder. Also included is a Rockwell Collins Multi-Function Radio set to coordinate the missions with possible ground troops, stranded victims, and with each other inside the aircraft. The SATCOM system covers needed long range communication requirements.

To give it the best chance of completing each mission successfully and, for medevac, as soon as possible, the Golden Retriever is equipped with the most up-to-date and efficient navigation systems. It features the Rockwell Collins Advanced Digital TACAN Receiver TCN-100, GPS, and low frequency direction finder. It also has a radar altimeter to record how far away the craft is from the ground directly beneath it so monitor the changes in the height of the terrain. The Rockwell Collins AN/ARN-147 (V) digital receiver that is compatible with the latest high-performance flight control systems, digital indicators, and



analog instruments. A personnel locator is used to support the combat search and rescue mission and provides covert location and extraction of downed pilots carrying survival radios.

The control systems and displays are made up of 4 Northrop Grumman All-Glass Cockpit Smart MFDs. The MFDs provide excellent visibility from every angle making it easy for both pilots to accurately read every screen. Also included in the control systems and display are FLIR, acoustic, and radar sensor videos equipped with electronic flight instrumentation and engine instrumentation.

In some missions it is essential for the vehicle to remain as aware of its surroundings as possible in order to survive in military scenarios. Although the heat signature is small already because of the ducted exhaust, further countermeasures have been taken as the Golden Retriever is equipped with Bae Systems AN/ALQ-144 onboard IR Jammer and with the option of outboard flare sets. It is also equipped with a Northrop Grumman AN/APR-39 Radar warning receiver integrated with missile and laser warning systems.

14. Cost Analysis

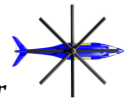
The most recent and similar craft to the Gold Retriever is the Sikorsky X-2, which is also a coaxial with a pusher prop. The total cost to purchase the Sikorsky X-2 would be between 4 and 5 million dollars if made for commercial purposes. The total production cost to develop the X-2 was around 50 million dollars.

The Bell PC Based Cost Model was used to calculate the total cost development of the Golden Retriever. Conservative values were used for the new technology and designs implemented. The total development cost of the Golden Retriever is \$40,588,000. The cost of the first prototype is estimated to be around \$7,000,000. Once the Golden retriever is in full production the cost will be \$5,583,000 The manufacturing material cost of the craft is around \$3,000,000. Table 20 below breaks down the total development cost of the Golden Retriever.

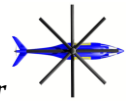
Table 20 Cost Analysis

Total Development Cost

Engineering	
Design	\$1,436,000
Flight Test	\$878,000
Component Test	\$3,530,000
Systems Engineering/Project Management	\$285,000
Total Engineering	\$6,129,000
Manufacturing Engineering	
Planning, Loft, Other	\$0
Project Management	\$0
Total Manufacturing Engineering	\$0



Tooling	
Tool Make	\$1,797,000
Outside Tooling	\$8,747,000
Total Tooling	\$10,544,000
Manufacturing	
Prototype (1)	\$7,003,000
No GTV, STA, or FTA required	\$0
Flight Test	\$1,346,000
Component Test	\$4,798,000
Total Manufacturing	\$13,147,000
Logistics	
	\$0
Other	
Travel and Per Diem	\$2,416,000
Direct Expense	\$8,352,000
Total Other	\$10,768,000
Total Program without profit	
	\$40,588,000
Profit @ 12.0%	\$4,871,000
Grand Total	\$45,459,000



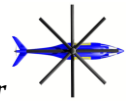
15. Conclusion

Designed as a true multi-mission capable aircraft, the Golden Retriever combines mature technologies into a high-performance platform pushing the boundaries of what is possible for modern VTOL aircraft. This is accomplished by utilizing technologies recently proven in rotorcraft and ready or near ready for production. Together these technologies allow the Golden Retriever to outperform virtually any existing traditional helicopter, redefining the role VTOL aircraft play in military and civil situations.

Center to the performance of the Golden Retriever is its co-axial rotor system. Modern materials and technologies have allowed us to push the time tested co-axial configuration to new levels of maneuverability while variable speed transmission allows for incredible speed. These gains are further realized due to reduced system weight from extensive use of composites as well as optimization of blade airfoil and fuselage shape. Performance is not achieved at the expense of safety though as structures have been designed for reliability, durability and crashworthiness as well as to reduce noise, both inside and out.

Truly, the technology present in the Golden Retriever allows it to accomplish its most important mission, saving lives, in a whole new way. Patients can be rushed directly to medical attention from over 225nm away in the critical golden hour, greatly increasing their chances of survival. Though this is the Golden Retriever's primary mission, another benefit of this aircraft is its versatility. The aircraft's reconfigurable cabin and excellent payload capability allows it to perform a wide variety of missions, taking the roles of multiple current aircraft, saving the operator space and money of having multiple single mission aircraft plus associated extra parts and additional costs.

In all, these technologies produce a versatile, high-performance package that fulfills multiple different missions including those previously thought impossible for a VTOL aircraft.



References

- Youngren, Harold. Kroninger, Chris. "Low Reynolds Number Testing of the AG38 Airfoil for the SAMARAI Nano Air Vehicle." AIAA-2008. January 10, 2008
- AERODYNAMIC FEATURES OF COAXIAL CONFIGURATION HELICOPTER. Eduard PETROSYAN, Deputy Chief Designer of Kamov Company.
- Yaw Moment Capability With Hingeless Rotors, May 26, 2005. (T-square)
- A Survey of Theoretical and Experimental Coaxial Rotor Aerodynamic Research. NASA Technical Paper 3675. 1997. Colin P. Coleman, Ames Research Center, Moffett Field, California
- Hill, P. & Peterson, C. (1992). Mechanics and thermodynamics of propulsion. New York, NY: Addison Wesley.
- Federation of American Scientist, RAH-66 Comanche. Retrieved from <http://www.fas.org/programs/ssp/man/uswpns/air/attack/rah66.html#infrared>
- Anderson, J.D. (2007). Fundamentals of aerodynamics. New York, NY: McGraw Hill.
- Prouty, R.W. (1990). Helicopter performance, stability and control. Malabar, Fla: Krieger.
- Oberg, Erik. Jones, Franklin. Horton, Holbrook. Ryffel, Henry. (2004). 27th Edition Machinery's Handbook. New York, New York: Industrial press Inc.
- 20 Oct 1989. Detailed Weight Statement (SES-700209). United Technologies.